

International Atomic Energy Agency

INDC(CCP)-320

Distr.: L

INDC

INTERNATIONAL NUCLEAR DATA COMMITTEE

TRANSLATION OF SELECTED PAPERS

PUBLISHED IN YADERNYE KONSTANTY (NUCLEAR CONSTANTS 3, 1987)

(Original Report in Russian was distributed
as INDC(CCP)-279/G)

Translated by the IAEA

December 1990

IAEA NUCLEAR DATA SECTION, WAGRAMERSTRASSE 5, A-1400 VIENNA



TRANSLATION OF SELECTED PAPERS
PUBLISHED IN YADERNYE KONSTANTY (NUCLEAR CONSTANTS 3, 1987)

(Original Report in Russian was distributed
as INDC(CCP)-279/G)

Translated by the IAEA

December 1990

Reproduced by the IAEA in Austria
January 1991

91-00134

Contents

Analysis of ^{235}U Neutron Cross-Sections in the Fast Neutron Energy Region By A.B. Klepatskij, V.A. Kon'shin, V.M. Maslov and E.Sh. Sukhovitskij	5
Energy Distributions of Secondary Neutrons for ^{235}U By V.A. Kon'shin, Yu.V. Porodzinskij and E.Sh. Sukhovitskij	17
Systematics of Radiation Widths and Level Density Parameters in the Mass Number Range Region $40 < A < 250$ By V.M. Bychkov, O.T. Grudzevich and V.I. Plyaskin	25
Integral Cross-Sections for the Reactions $^{51}\text{V}(n,\alpha)^{48}\text{Sc}$, $^{93}\text{Nb}(n,2n)^{92}\text{Nb}^m$ and $^{90}\text{Zr}(n,2n)^{89}\text{Zr}$ By E.I. Grigor'ev, Yu.A. Melekhin and V.P. Yaryna	41
Approximation of the Cross-Sections for Charged- Particle Emission Reactions near the Threshold By S.A. Badikov and A.B. Pashchenko	45
Group Constants for ^{233}U , ^{235}U and ^{239}Pu in the Resonance Region By A.A. Van'kov, V.V. Kolesov and V.F. Ukraintsev	55

ANALYSIS OF ^{235}U NEUTRON CROSS-SECTIONS IN THE FAST NEUTRON ENERGY REGION

A.B. Klepatskij, V.A. Kon'shin, V.M. Maslov, E.Sh. Sukhovitskij

The need to carry out evaluation of the whole system of nuclear data for ^{235}U has arisen as a result of the appearance of new experimental data and the establishment of more accurate theoretical models for calculating neutron cross-sections [1]. New experimental results have appeared on the fission cross-section, the total cross-section and the α parameter. In the low energy region, experimental data on the fission cross-section classified according to the spin of the compound nucleus have been obtained, and this has made it possible to resolve a large number of close resonances. Progress in the theoretical interpretation of neutron cross-sections has allowed evaluation of nuclear data using the coupled channel method (even for nuclei with large ground state spin values), correct level density and transient fission state models, and the multiscascade statistical model taking into account the possibility of pre-equilibrium decay.

The present work focuses on the specific aspects of evaluating neutron data in the fast neutron energy region. Emphasis is placed on the evaluation of those types of cross-section for which few experimental data are available or where the data are contradictory.

The total interaction cross-section and the potential and direct inelastic scattering cross-sections have been evaluated on the basis of calculations using the coupled channel method with the potential obtained for the actinide group [2]. Taking into account the proposed isotopic dependence, the potential parameters for ^{235}U are:

$$\begin{aligned} V_R &= 46,03 - 0,3E; \quad \tau_R = 1,256 \text{ fm}; \quad \alpha_R = 0,626 \text{ fm}; \\ W_0 &= \begin{cases} 3,05 + 0,4E & (E \leq 10 \text{ MeV}), \\ 7,05 & (E > 10 \text{ MeV}), \end{cases} \quad \tau_D = 1,260 \text{ fm}; \\ V_{S0} &= 7,5 \text{ MeV}; \quad \beta_2 = 0,201; \quad \beta_4 = 0,072. \end{aligned}$$

The calculations took into account the coupling between five levels of the main rotation band at energies close to 3 MeV, while at higher energies

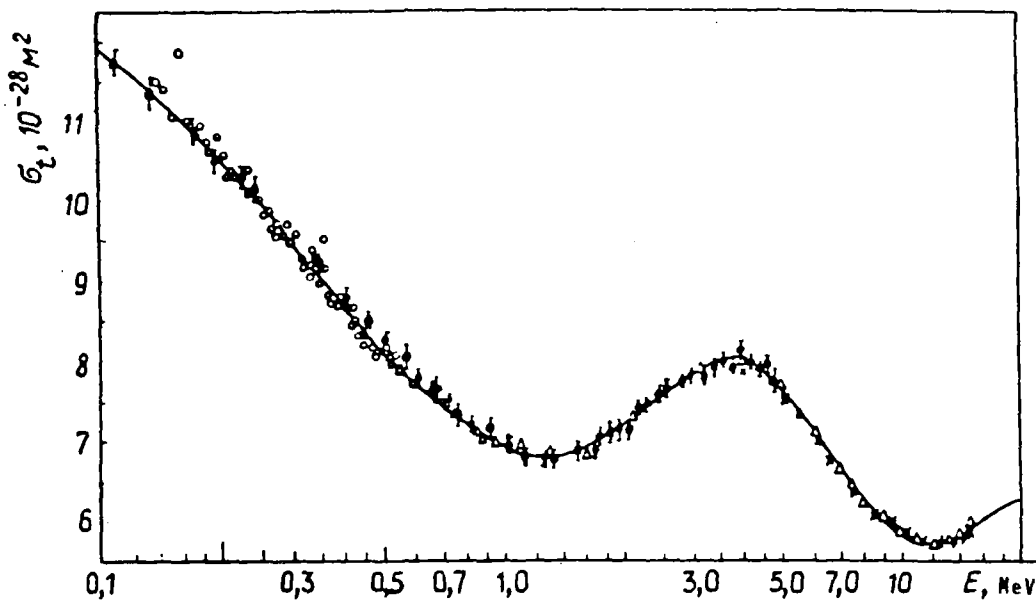


Fig. 1. Comparison of theoretical (continuous curve) and experimental (I - [3]; Δ - [4]; X - [5]; O - [6]) cross-sections σ_t for ^{235}U in the 0.1-20 MeV energy range.

they were performed in the adiabatic approximation. At the same time, the neutron transparencies needed for calculations using the statistical model were obtained. Calculated and experimental [3-6] data on the total cross-section σ_t for ^{235}U are shown in Fig. 1. The discrepancy between the theoretical and experimental cross-sections is no more than 2%, which is within the error of the evaluated curve. In Figs 2-4 a comparison is made between experimental and theoretical (calculated using the coupled channel method and the statistical model) integral elastic interaction cross-sections and scattered neutron angular distributions. From Fig. 2 it can be seen that the earlier data on the measurement of the elastic scattering cross-section [7, 8], obtained in experiments with inadequate energy resolution, contain a contribution from inelastic scattering of neutrons at low-lying levels. This contribution amounts to about 10% in the energy region up to 2 MeV and about 5% in the 3-20 MeV region. Figure 3 shows good agreement with the experimental data, thus bearing witness to the accuracy of the direct and compound process calculations, since at 0.7 MeV the contribution from processes involving the formation of a compound nucleus is significant (for the

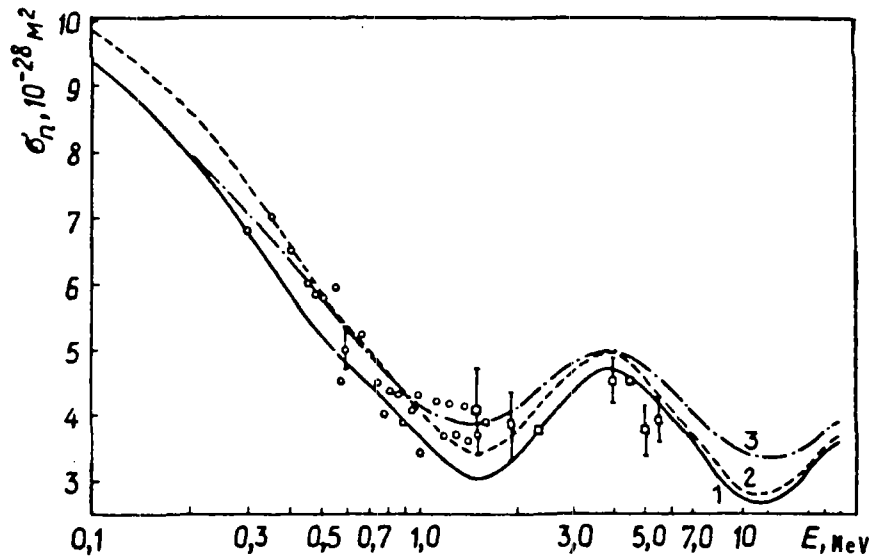


Fig. 2. Comparison of theoretical and experimental (\square - [7]; \circ - [8]) integral cross-sections for elastic scattering of neutrons by the ^{235}U nucleus in the 0.1-20 MeV energy range: 1 - calculation for the ground state ($7/2^-$); 2 - calculation for the ground state taking into account the contribution of inelastic scattering at the first five levels (73 eV, 13, 46, 52 and 82 keV); 3 - ENDF/B-V evaluation [9].

46 keV level, $\sigma_{\text{comp}} = 0.168 \times 10^{-28} \text{ m}^2$, $\sigma_{\text{dir}} = 0.143 \times 10^{-28} \text{ m}^2$,

whereas at 3.4 MeV it is less than 0.02%. From Fig. 4 it can be seen that the data on the angular distributions of elastically scattered neutrons [11], obtained with low energy resolution, may be analysed only by taking into account the contribution from inelastic scattering of neutrons at low levels (at least two-three). Therefore evaluations based on Legendre polynomial expansion of the experimental data as a rule significantly underestimate the anisotropy of elastic scattering.

The generalized optical model of the nucleus involves a change in the neutron transparency coefficients for various partial waves. The accuracy of the neutron transparency calculation affects primarily the value of the compound nucleus formation cross-section, and consequently the reliability of the calculation and evaluation of the inelastic scattering cross-section, both the total cross-section and the cross-sections at the individual levels.

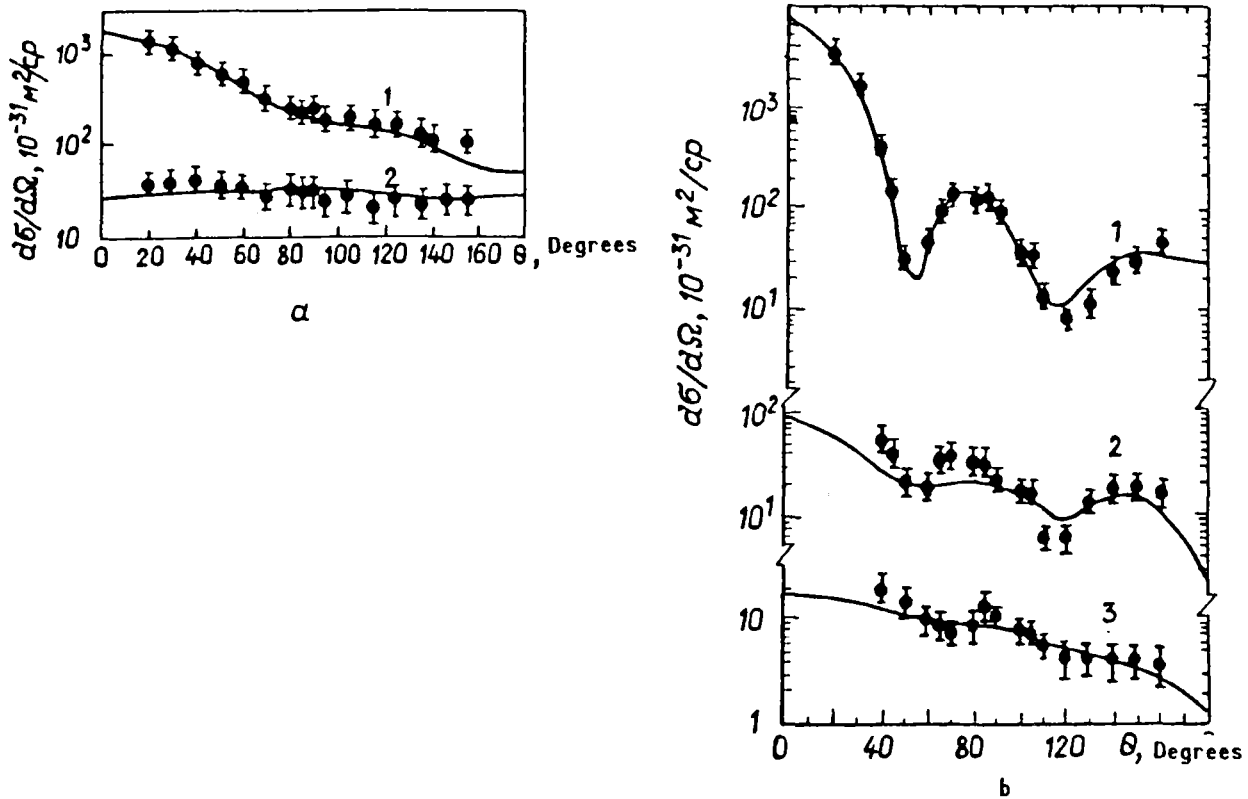


Fig. 3. Comparison of theoretical (continuous curve) and experimental data (● - [10]) on the angular distribution of scattered neutrons for ^{235}U at 0.7 MeV(a) and 3.4 MeV(b) for the levels $7/2^-$ - ground state; $1/2^+$ - 73 eV, $3/2^+$ - 13 keV (curve 1); $9/2^-$ - 46.2 keV; $5/2^+$ - 51.7 keV (curve 2) and for the level $11/2^-$ - 103 keV (curve 3).

In calculating the cross-sections for inelastic scattering of ^{235}U using the statistical model, neutron transparency coefficients computed by the coupled channel method were employed. In the region of energies greater than the highest discrete level (426.7 keV), a continuous level spectrum was used. In order to predict the level density energy dependence in the neutron channel and the transient fission states, the superfluid model of the nucleus taking into account collective effects was used [12]. Such an approach made possible a good description of the experimental data on the excitation cross-sections for discrete levels of ^{238}U and ^{239}Pu [1] and was therefore also used for ^{235}U .

The main difficulty in experiments to measure the neutron inelastic scattering cross-section for ^{235}U lies in the subtraction of the fission

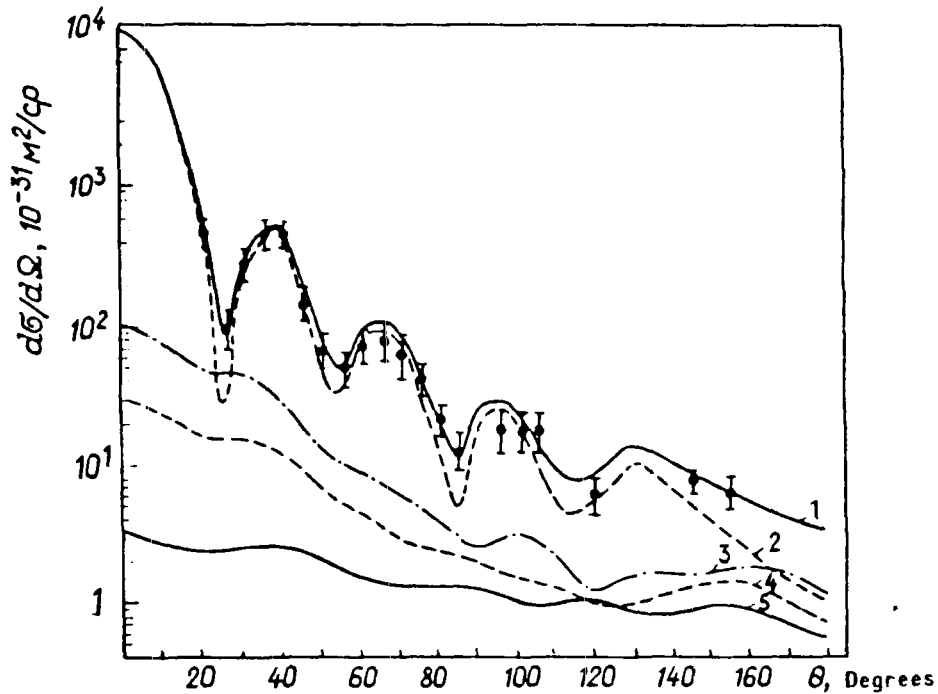


Fig. 4. Comparison of theoretical and experimental (● - [11]) data on the angular distribution of scattered neutrons for ^{235}U at 14 MeV. Results of the present calculations: curve 1 - sum of levels ($7/2^-$ - ground state; $9/2^-$ - 46.2 keV; $11/2^-$ - 103 keV; $13/2^-$ - 170.7 keV); curve 2 - level $7/2^-$; curve 3 - $9/2^-$; curve 4 - $11/2^-$; curve 5 - $13/2^-$.

spectrum from the total spectrum and the subtraction of inelastic contributions of low-lying levels from the elastic peak. The authors of Ref. [13] determined the neutron inelastic scattering cross-section for ^{235}U level groups in an experiment where the energy resolution was not high enough. Figure 5 shows a comparison of the experimental data [7, 13, 14] with the theoretical data obtained by us for three level groups. It can be seen from the diagram that the theoretical and the available integral experimental data agree to within the limits of the experimental error. It is difficult to make a more detailed comparison because of the low energy resolution of the experiment in Ref. [13] (it is not clear, for example, whether the 150.5 keV level was included in the experimentally measured cross-section $\sigma_{nn'}$ for the level group $100 < Q < 150$ keV). As yet, it is difficult to draw any definitive conclusions regarding the efficiency of the theoretical model used to calculate the cross-section $\sigma_{nn'}$, since no experimental data

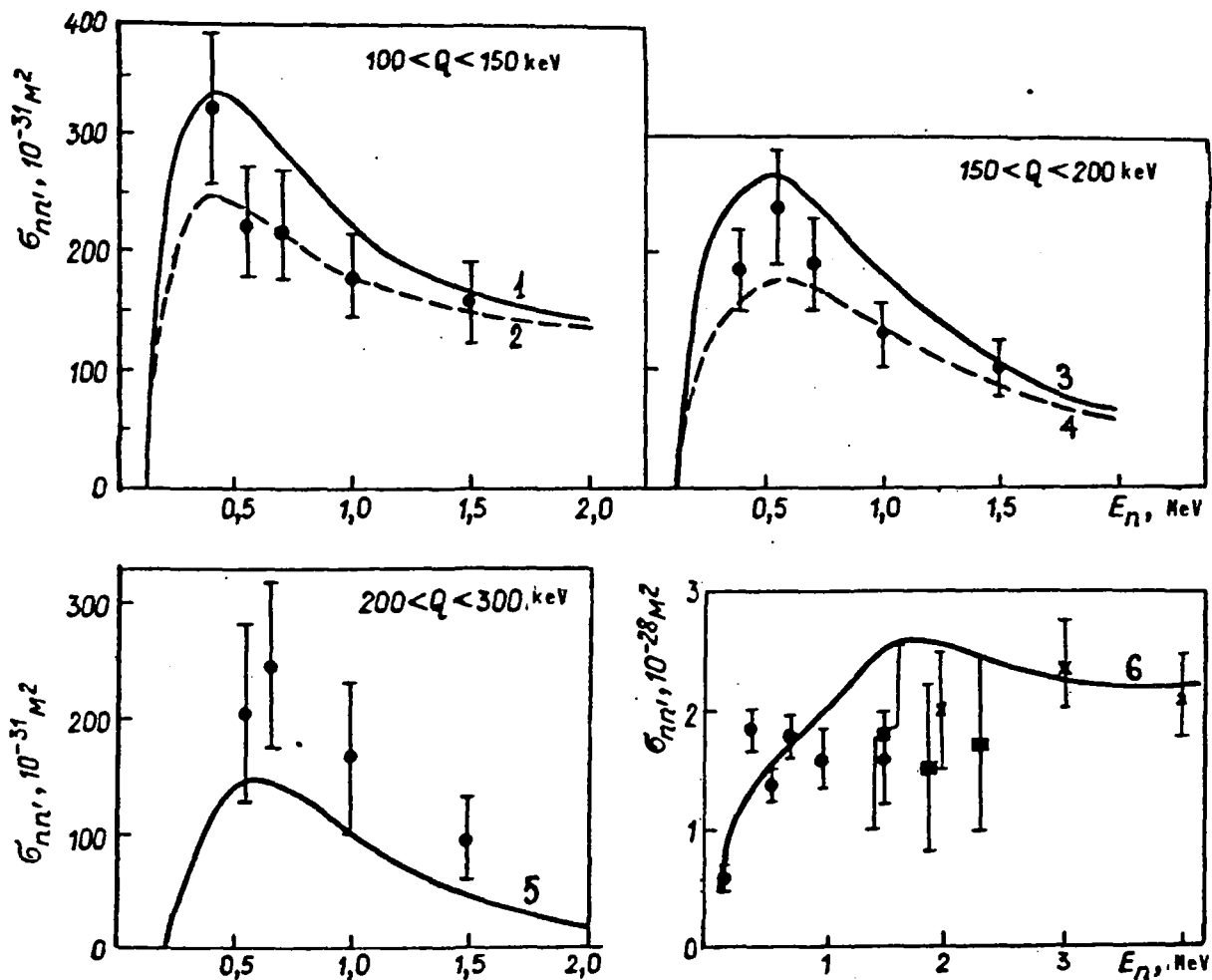


Fig. 5. Comparison of theoretical and experimental (■ - [7], ● - [13] x - [14]) data on the excitation of ^{235}U level groups for neutron inelastic scattering. Sum of levels: curve 1 - 103, 129.3 and 150.5 keV; curve 2 - 103 and 129.3 keV; curve 3 - 170.7, 171.4, 197.1 and 150.5 keV; curve 4 - 170.7 and 197.1 keV; curve 5 - 225.4, 291.1 and 294.7 keV; curve 6 - total inelastic scattering cross-section.

are available on the excitation functions for the individual levels of ^{235}U in neutron inelastic scattering. Note that the inelastic scattering cross-sections $\sigma_{nn'}$, calculated by the authors in the 1-2.5 MeV region are somewhat higher than the experimental data [7, 13] obtained with poor energy resolution (curve 6, Fig. 5), which confirms the assumption made above that the contribution from low-lying levels was included in the elastic scattering in these experiments.

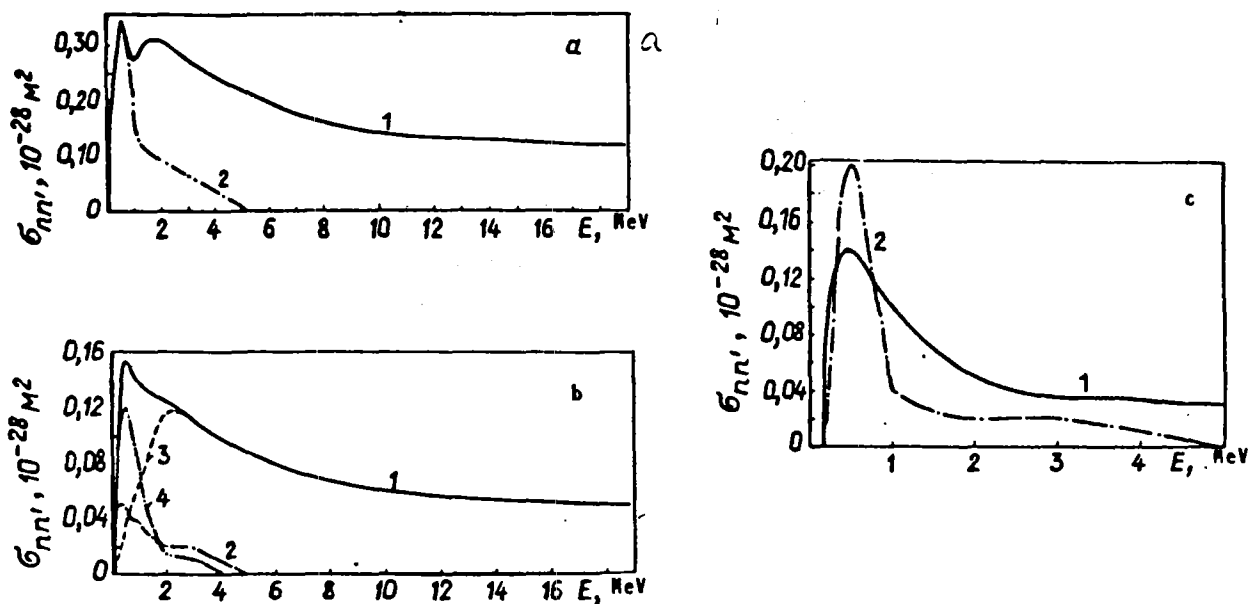


Fig. 6. Comparison of the results of the present calculations (curves 1, 3 and 4) with ENDF/B-V data [9] (curve 2) on the excitation functions for the levels 46.21 (a), 103.03 (b) and 170.73 + 171.36 (c) in neutron inelastic scattering (3 - direct excitation process; 4 - compound process).

Comparison of the results of the present work with ENDF/B-V data [9] (Fig. 6) on level excitation functions shows considerable discrepancy, due to the fact that the contribution of direct processes was not taken into account in Ref. [9]. In that evaluation, the level 170.73 keV is not included and the excitation cross-section for the level 172 keV evidently includes the excitation cross-section for the two levels (170.73 and 171.36) in our evaluation. In addition, there are also discrepancies in the calculated compound contributions to the level excitation functions arising from the insufficiently accurate methods used in Ref. [9] to calculate the cross-section $\sigma_{nn'}$ from the energy-level diagram and for the method of taking into account fission competition. Naturally, the discrepancies in the level excitation cross-sections also affect the total inelastic scattering cross-section (Fig. 7). The results of the present work and the ENDF/B-V evaluation [9] for the cross-section $\sigma_{nn'}$ vary by a factor of 1.5-2. The majority of discrepancies in the 0.1-5.0 MeV region result from taking into account the contribution of direct processes to the low-lying states of ^{235}U , which was disregarded in

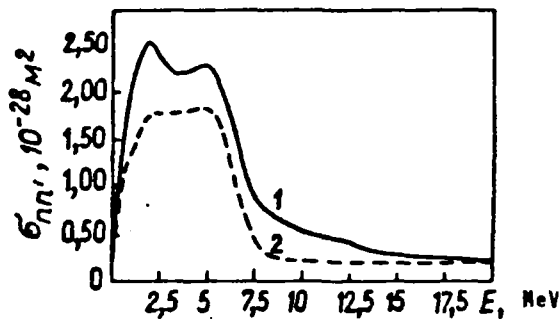


Fig. 7. Total neutron inelastic scattering cross-section for ^{235}U from the threshold to 20 MeV: 1 - result of the present work; 2 - ENDF/B-V [9].

the ENDF/B-V evaluation. In the energy region above 7 MeV, the higher value for the cross-section σ_{nn} , obtained in the present work is accounted for by the fact that pre-equilibrium processes were included in our evaluation. Both these effects lead to hardening of the emitted neutron spectrum.

There are few experimental data on the cross-sections for the (n,2n) and (n,3n) reactions [15-17], and those that are available are contradictory. The problem of evaluating the cross-sections for these reactions can be solved by using a consistent description of the cross-sections for fission and for the (n,2n) and (n,3n) reactions. In this endeavour, the correct determination of the contributions to the total fission cross-section from emissive fission in reactions of the type (n,xnf), where $x = 1, 2 \dots$, calls for a knowledge not only of the fissilities of the corresponding nuclei, but also of the spectrum of inelastically scattered neutrons.

The results of Ref. [18] were used to determine the fissilities of the nuclei. These results show that, if collective, superfluid and shell effects exerted on the level densities by equilibrium-deformed and severely deformed states, and also by deformations disrupting the mirror symmetry of the fissile nucleus in saddle configurations, are taken into account, it is possible, in the double-peaked fission barrier model, to reproduce the energy dependence of the experimental fission cross-sections for uranium and plutonium isotopes in the region of the first "plateau".

The availability of experimental data on all types of neutron cross-section above the threshold of the (n,n'f) reaction and on the secondary neutron spectra for ^{238}U gives the unique opportunity of making a consistent description of the cross-sections for the reactions (n,F), (n,2n) and (n,3n) in the neutron energy region up to 20 MeV. The parametrization of the secondary neutron spectra for ^{238}U within the framework of the pre-equilibrium decay model made it possible to reproduce the fission cross-section in the energy region 1-20 MeV and, consequently, to evaluate the cross-sections for (n,xn) reactions. The conditions for the optimum description of the hard part of the spectra for ^{238}U were used to determine [19] the main parameter of the pre-equilibrium decay model (a two-particle interaction matrix element equal to $10/A^3$) which was used for ^{235}U . In order to describe the cross-sections close to the thresholds, the level density in the neutron and fission channels was approximated by a constant temperature model, the parameters of which were determined from the condition for a smooth "seam" with the super-fluid nucleus model [12].

Such an approach made it possible to reproduce the cross-section σ_{nF} to within the limits of the errors in the experimental data for virtually the whole of the energy region examined (Fig. 8). Evaluations of the behaviour of the cross-section for the first "chance" fission, σ_{nf} [9, 20], and consequently, other "chances" are very contradictory and at energies greater than the threshold for the (n,n'f) reaction differ by several times. The slight decrease in our calculation of the cross-section σ_{nf} can be explained by the increase in the contribution of the non-equilibrium component to the inelastically scattered neutron spectrum.

Figure 9 provides a comparison of the evaluated cross-sections for the (n,2n) and (n,3n) reactions with experimental data renormalized to take account of contemporary standards for the cross-section σ_{nF} for ^{235}U and ^{238}U and for the number $\bar{\nu}_p$ for ^{252}Cf . As can be seen from Fig. 9, our evaluation of the cross-section $\sigma_{n,2n}$ agrees well with the experimental

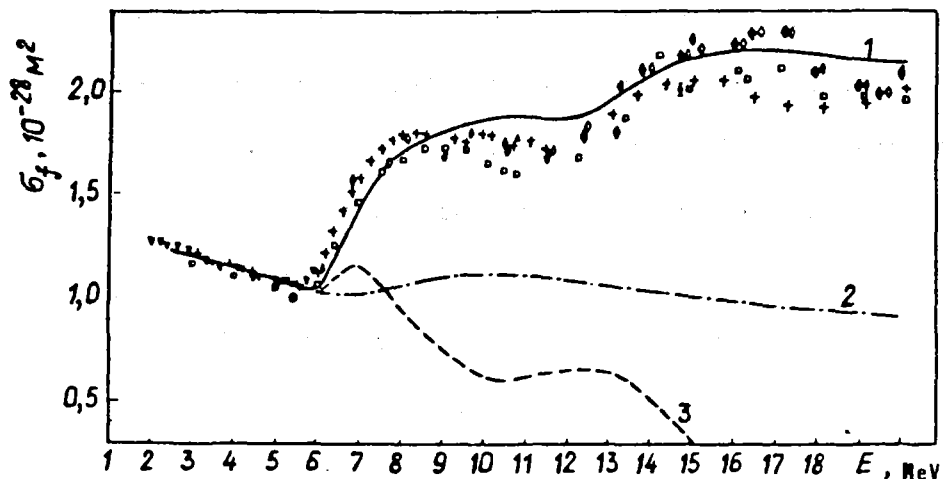


Fig. 8. Comparison of theoretical and experimental (taken from Ref. [1]) data on the fission cross-section for ^{235}U . Calculations of the present work: 1 - fission cross-section; 2 - cross-section for first "chance" of fission. Curve 3 - evaluation of the first "chance" of fission, obtained in Ref. [20].

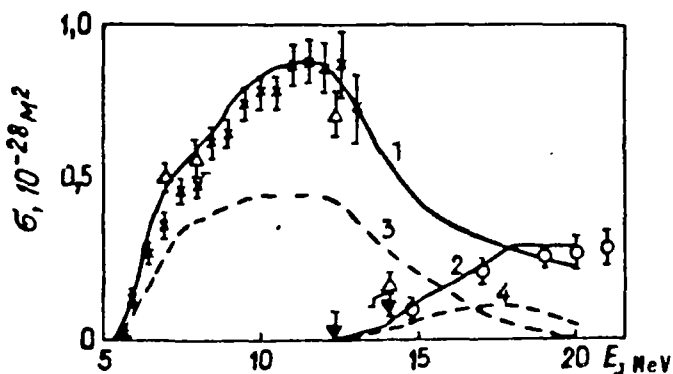


Fig. 9. Comparison of the evaluated cross-sections for (n,2n) reactions (curves 1 and 3) and (n,3n) reactions (curves 2 and 4) from the present work (curves 1 and 2) and from ENDF/B-V [9] (curves 3 and 4) with the experimental data: Δ - $\sigma_{n,2n}$ [15]; ∇ - $\sigma_{n,2n}$ [17]; \circ - $\sigma_{n,3n}$ [15]; ϕ - $\sigma_{n,3n}$ [16]

data of Refs [17] and [15], with the exception of the point 14 MeV, and the evaluation of the cross-section $\sigma_{n,3n}$ agrees well with the data in Ref. [16]. The ENDF/B-V evaluation [9] for the cross-sections $\sigma_{n,2n}$ and $\sigma_{n,3n}$ does not agree with the available experimental data.

Full data on the evaluated cross-sections σ_t , σ_n , $\sigma_{n\gamma}$, $\sigma_{nn'}$, $\sigma_{nn'}(E_q)$, σ_f , $\sigma_{n,2n}$, $\sigma_{n,3n}$, and $\bar{\nu}_t$, the angular distributions of

elastically and inelastically scattered neutrons, and the secondary neutron spectra are contained in Ref. [1].

In view of the above, it may be concluded that the whole system of evaluated nuclear data for ^{235}U in the energy region from 10^{-5} eV to 20 MeV [1] has been established by means of correct theoretical models implementing modern physical concepts and taking into account all the available experimental results.

REFERENCES

- [1] KON'SHIN, V.A., ANTSIPOV, G.V., SUKHOVITSKIJ, E.Sh., et al., Evaluated Neutron Constants for ^{235}U , Nauka i tekhnika, Minsk (1985) [in Russian].
- [2] KLEPATSKIJ, A.B., KON'SHIN, V.A., SUKHOVITSKIJ, E.Sh., The coupled channel method and the evaluation of neutron data for fissionable nuclei, Izv. Akad. Nauk BSSR - Ser. Fiz.-Ehnerg. Nauk 2 (1984) 21-29 [in Russian].
- [3] POENITZ, W.R., WHALEN, J.F., SMITH, A.B., Total neutron cross-sections of heavy nuclei. In: Nucl. Data for Technol. (Proc. Int. Conf. Knoxville, 1979), Washington (1980) 698-704.
- [4] SCHWARTZ, R.B., SCHRACK, R.A., HEATON, H.T., Total neutron cross-sections of ^{235}U , ^{238}U , ^{239}Pu from 0.5 to 15 MeV. Nucl. Sci. Eng. 54 (1974) 322-326.
- [5] FOSTER, D.G., Jr., GLASGOW, D.W., Total neutron cross-sections at 2.5-15.0 MeV. 1. Exp. Phys. Rev. C3 (1971) 576-603.
- [6] CABE, I., CANCE, M., ADAM, A. et al., Mesure des sections efficaces totales neutroniques du carbone, du nickel, de ^{235}U , ^{238}U , ^{239}Pu entre 0.1 MeV et 6 MeV, In: Nucl. Data for Reactors (Proc. Int. Conf. Helsinki, 1970) Vol. II, IAEA, Vienna (1970) 31-37.
- [7] KNITTER, H.H., ISLAM, M.M., COPPOLA, M., Investigation of fast neutron interaction with ^{235}U . Z. Physik 257 (1972) 108-123.
- [8] SMITH, A.B., Elastic scattering of fast neutrons from ^{235}U . Nucl. Sci. Eng. 18 (1964) 126-129.
- [9] BHAT, M.R., Evaluated nuclear data file/B, version V, MAT 1395 (1977).
- [10] HAOUAT, G., LACHKAR, J., LAGRANGE, Ch. et al., Neutron scattering cross-sections for ^{232}Th , ^{233}U , ^{235}U , ^{238}U , ^{239}Pu and ^{242}Pu between 0.6 and 3.4 MeV. Nucl. Sci. Eng. 81 (1982) 491-511.
- [11] KAMMERDIENER, I., Neutron spectra emitted by ^{239}Pu , ^{238}U , ^{235}U , Pb, Nb, Ni, Al and C irradiated by 14 MeV neutrons: Rep. UCRL-51232, Livermore (1972).

- [12] IGNATYUK, A.V., ISTEKOV, K.K., SMIRENKIN, G.N., Role of collective effects in the systematics of nuclear level densities, *Yadernaya fizika* 29 (1979) 875-883 [in Russian].
- [13] ARMITAGE, B.H., FERGUSON, A.T.G., MONTAGUE, J.H. et al., Inelastic scattering of fast neutrons by ^{235}U . In: *Nucl. Data for Reactors* (Proc. Int. Conf. Paris, 1966) IAEA, Vienna (1967) 383-392.
- [14] BATCHELOR, R., WYLD, K., Neutron scattering by ^{235}U and ^{239}Pu for incident neutrons of 2.3 and 4 MeV: Rep. AWRE-055/69 Aldermaston (1969).
- [15] MATHER, D.S. et al., Measurement of (n,2n) cross-sections for incident energies between 6 and 14 MeV: Rep. UKAEA, AWRE-0-72/72 (Nov. 1972).
- [16] VEESER, L.R., ARTHUR, E.D., In: Measurements of (n,3n) cross-sections for ^{235}U and ^{238}U neutron physics and nuclear data: Proc. Int. Conf. Harwell, 1978), OECDNEA (1978) 1054-1058.
- [17] FREHAUT, J., BERTIN, A., BOIS, R., Measurement of the ^{235}U (n,2n) cross-section between threshold and 13 MeV. *Nucl. Sci. Eng.* 74 (1980) 29-33.
- [18] IGNATYUK, A.V., KLEPATSKIJ, A.B., MASLOV, V.M., SUKHOVITSKIJ, E.Sh., Analysis of fission cross-sections for U and Pu isotopes by neutrons in the first "plateau" region, *Yad. Fiz.* 42 3(9) (1985) 569-577 [in Russian].
- [19] GRUDZEVICH, O.T., IGNATYUK, A.V., MASLOV, V.M., PASHCHENKO, A.B., Consistent description of cross-sections for the (n,n'f) and (n,xn) reactions for transuranium nuclei. In: *Nejtronnaya Fizika* (Proc. Sixth All-Union Conf. on Neutron Physics, Kiev, 2-6 October 1983), Vol. 2, TsNIIatominform, Moscow (1984) 318-323.
- [20] MADLAND, D.G., NIX, J.R., New calculation of prompt fission neutron spectra and average prompt neutron multiplicities. *Nucl. Sci. Eng.* 81 (1982) 213-271.

ENERGY DISTRIBUTIONS OF SECONDARY NEUTRONS FOR ^{235}U

V.A. Kon'shin, Yu.V. Porodzinskij, E.Sh. Sukhovitskij

Reference [1] demonstrates that a self-consistent description of the reactions $(n,2n)$, $(n,3n)$, (n,xnf) and of the total neutron spectra of these reactions for ^{238}U and ^{235}U is possible using a theoretical model incorporating such features as accurate calculation of neutron transparencies and, consequently, of the compound nucleus formation cross-section, allowance for pre-equilibrium emission of neutrons, and calculation of the level density in the neutron and fission channels within the framework of a superfluid nucleus model taking into account shell and collective effects.

However, the program embodying the described model [2] is not able to predict the spectra of each of the sequentially emitted neutrons for specific reactions: it only gives the total neutron spectra for the reactions (n,n') and (n,xn) .

Therefore, with a view to calculating the energy dependences of secondary neutrons in specific reactions, a simple model was developed which makes no allowance for dependence on spin J , but does permit the neutron spectra for these reactions to be obtained. The first neutron spectrum for the reaction (n,xn) was found by summation of the pre-equilibrium neutron emission spectrum determined by the exciton model [3] and the equilibrium neutron spectrum determined as in Ref. [4]

$$I_p^{(1)}(E_n, E') = E' \sigma_c(E_n, E') \rho(E_n - B_n - E'),$$

where E_n is the energy of the incident neutron; E' is the energy of the emitted neutron; $\sigma_c(E_n, E')$, is the cross-section for the inverse reaction to neutron emission; ρ is the state density of the residual nucleus; and B_n is the neutron separation energy.

The total first neutron spectrum is the sum of the pre-equilibrium and equilibrium spectra in specific proportions. The relative proportions of the

pre-equilibrium part of the spectrum and the compound cross-section are determined using the two-particle interaction matrix element M^2 , which is equal to $10/A^3$ [5]. This spectrum defines the excitation distribution for residual nuclei after emission for the first neutron $\chi^1(E)$. It is not difficult to obtain the nucleus excitation probability distribution after emission of the $(n + 1)$ -th neutron:

$$\chi^{n+1}(E) = \int_{E+B_n}^{E_n} \chi^n(E') S^A(E', E) dE',$$

where $S^A(E', E)$ is the probability that a nucleus A with an excitation E' will emit a neutron of energy $E' - E - B_n$ and turn into a nucleus A-1 with excitation E.

The probability $S^A(E', E)$ is normalized using the condition

$$\int_0^{E' - B_n} S^A(E', E) dE = \frac{\Gamma_n^A(E')}{\Gamma^A(E')},$$

where $\Gamma_n^A(E')$ and $\Gamma^A(E')$ are the neutron and total widths.

Assuming that the second and subsequent neutrons are emitted from the equilibrium state, the spectrum $I_p^{(1)}$ defines $S^A(E', E)$ to within the accuracy of the normalization $f(E')$:

$$S^A(E', E) = f(E') \sigma_c(E' - B_n - E)(E' - B_n - E) \rho(E),$$

where

$$f(E') = \frac{\Gamma_n^A(E')}{\Gamma^A(E') \int_0^{E' - B_n} \sigma_c(E' - B_n - E)(E' - B_n - E) \rho(E) dE},$$

allowing for $\sigma_c(E, E') = \sigma_c(E')$.

The spectrum of the second neutron in the reaction $(n, 2n'x)$ was determined using the formula

$$I^{(2)}(E_n, E') = \int_{B_n^A + E'}^{E_n} \chi^1(\varepsilon) S^A(\varepsilon, \varepsilon - B_n^A - E') d\varepsilon.$$

The spectrum of the third neutron in the reaction $(n,3n'x)$ was determined as follows

$$I^{(3)}(E_n, E') = \int_{B_n^{A-1} + E'}^{E_n - B_n^A} \chi^{(2)}(\varepsilon) S^{A-1}(E, \varepsilon - B_n^{A-1} - E') d\varepsilon.$$

The spectrum of the reaction $(n,n'\gamma)$ was determined thus

$$I_{nn'}(E_n, E') = I^{(1)}(E_n, E') \frac{\Gamma_\gamma^A(E_n - E')}{\Gamma^A(E_n - E')}.$$

The spectrum of the first neutron in the reaction $(n,2n)$ was found using the formula

$$I_{n,2n}^{(1)}(E_n, E') = I^{(1)}(E_n, E') P_1(E_n, E_n - E'),$$

where

$$P_1(E_n, E_n - E') = \begin{cases} 0, & \text{if } E' > E_n - B_n^A; \\ \int_0^{E_n - E' - B_n^A} S^A(E_n - E', \varepsilon) \frac{\Gamma_\gamma^{A-1}(\varepsilon)}{\Gamma^{A-1}(\varepsilon)} d\varepsilon, & \text{if } E' < E_n - B_n^A, \end{cases}$$

and the spectrum of the second neutron in the reaction $(n,2n)$, using the following expression

$$I_{n,2n}^{(2)}(E_n, E') = \int_{E' - B_n^A}^{E_n} \chi^1(\varepsilon) S^A(\varepsilon, \varepsilon - B_n^A - E') \frac{\Gamma_\gamma^{A-1}(\varepsilon - B_n^A - E')}{\Gamma^{A-1}(\varepsilon - B_n^A - E')} d\varepsilon.$$

Analogous expressions can be written for the spectra of the sequentially emitted neutrons from the reactions $(n,3n)$, $(n,n'f)$, $(n,2n'f)$, etc. The total secondary neutron spectra and the contributions of the reactions (n,n') , $(n,2n)$, $(n,3n)$, $(n,n'f)$, $(n,2n'f)$ according to the above model agree with the results of calculations by the STAPRE program [2] using a level density from a Fermi-gas model with a fundamental parameter a , some 20% higher than the value used in Ref. [1]. Fission widths in the fast energy region were determined from the relationship of the fission cross-section to

the compound nucleus formation cross-section (the latter being calculated by the coupled channel method). In this way, it proved possible to use the above model to calculate partial secondary neutron spectra.

The results of calculating spectra for secondary neutrons emitted in the reactions (n,2n), (n,3n) and (n,n') for ^{235}U are given in Figs 1-4. No

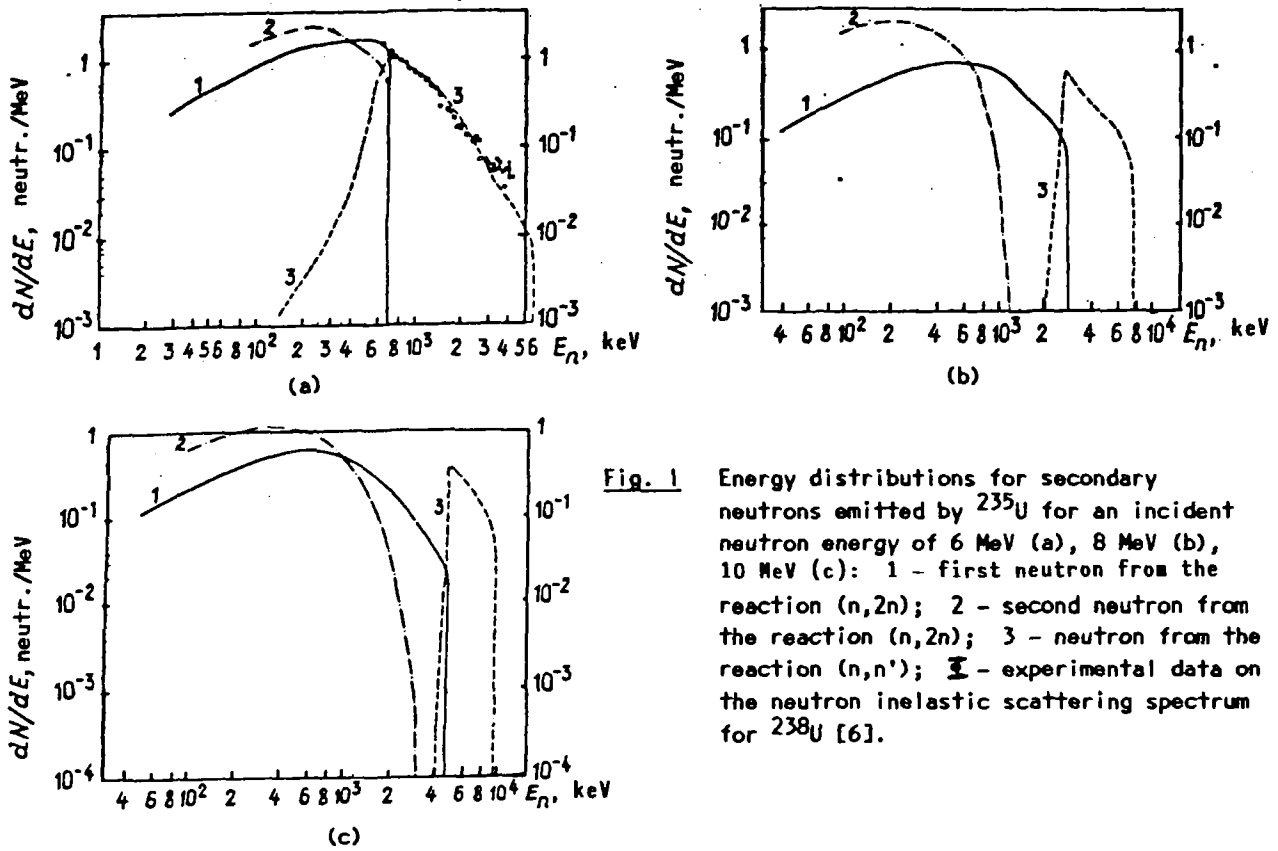


Fig. 1 Energy distributions for secondary neutrons emitted by ^{235}U for an incident neutron energy of 6 MeV (a), 8 MeV (b), 10 MeV (c): 1 - first neutron from the reaction (n,2n); 2 - second neutron from the reaction (n,2n); 3 - neutron from the reaction (n,n'); --- - experimental data on the neutron inelastic scattering spectrum for ^{238}U [6].

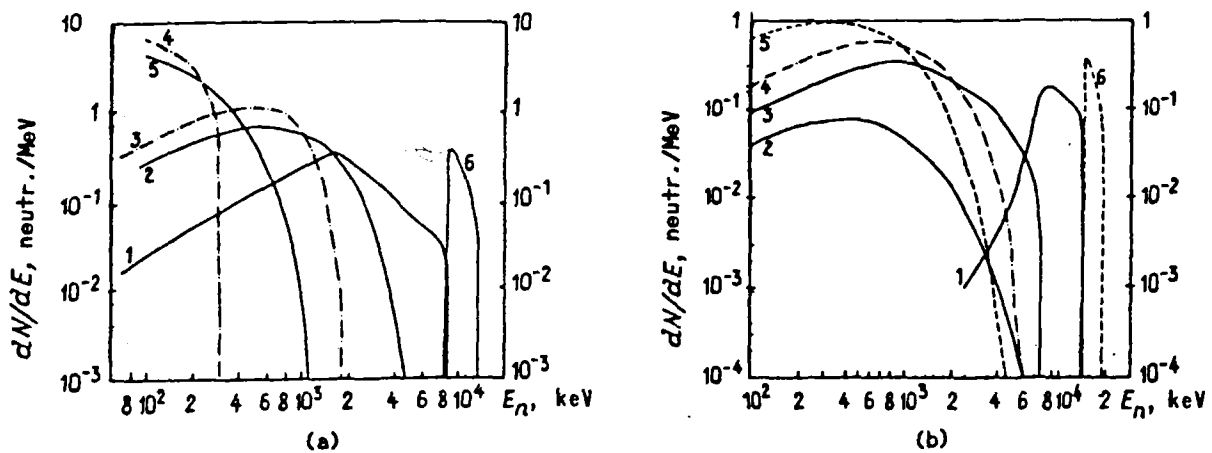


Fig. 2 Energy distributions of secondary neutrons emitted by ^{235}U for an incident neutron energy of 14 MeV (a) and 20 MeV (b): 1, 2 - first and second neutrons from the reaction (n,2n) respectively; 3, 4 - first and second neutrons from the reaction (n,3n) respectively; 5 - third neutron from the reaction (n,3n); 6 - neutron from the reaction (n,n').

Fig. 3 Energy distributions of first neutrons emitted by ^{235}U for an incident neutron energy of 8 MeV: 1 - neutron from the reaction (n,n') ; 2 - first neutron from the reaction $(n,2n)$; 3 - neutron from the reaction $(n,n'f)$; 4 - total first neutron spectrum.

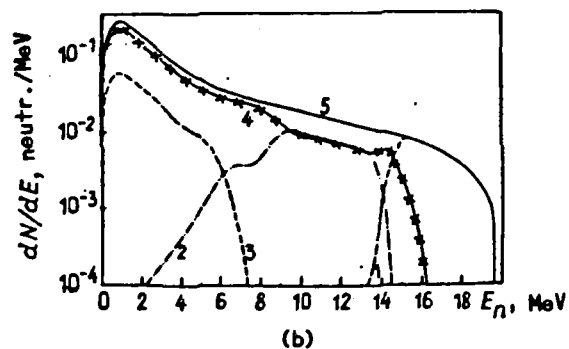
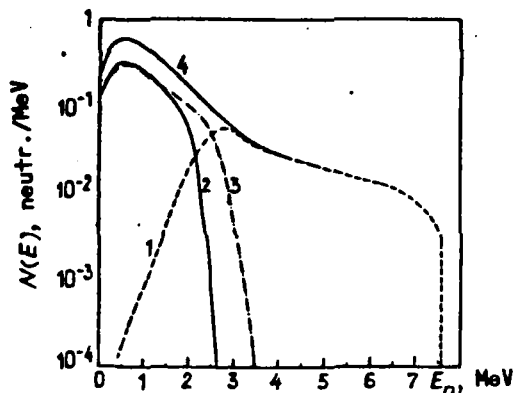
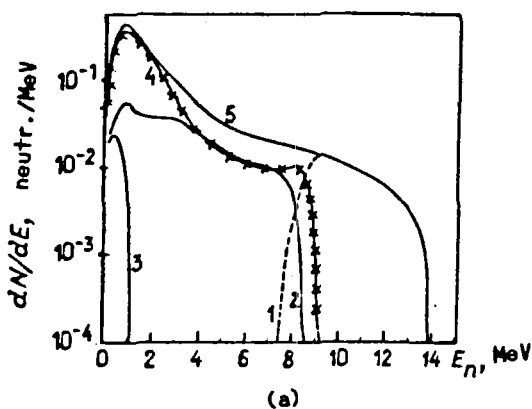


Fig. 4 Energy distributions of first neutrons emitted by ^{235}U for an incident neutron energy of 14 MeV (a), 20 MeV (b): 1 - neutron from the reaction (n,n') ; 2 - first neutron from the reaction $(n,2n)$; 3 - first neutron from the reaction $(n,3n)$; 4 - spectrum of first neutrons from the reactions $(n,n'f)$ and $(n,2nf)$ [and the reaction $(n,3nf)$ in Fig. 4(b)]; 5 - total first neutron spectrum.

Table

Mean energy values \bar{E} of secondary neutrons for ^{235}U

Incident neutron energy, MeV	\bar{E} , MeV					
	First neutron from the reaction $(n,2n)$	Second neutron from the reaction $(n,2n)$	First neutron from the reaction $(n,3n)$	Second neutron from the reaction $(n,3n)$	Third neutron from the reaction $(n,3n)$	Neutron from the reaction (n,n')
0,5	-	-	-	-	-	0,05
1,0	-	-	-	-	-	0,29
2,0	-	-	-	-	-	0,55
3,0	-	-	-	-	-	0,69
4,0	-	-	-	-	-	0,83
6,0	0,40	0,31	-	-	-	1,45
8,0	1,03	0,36	-	-	-	4,13
10,0	1,34	0,68	-	-	-	6,42
12,0	1,76	0,89	-	-	-	8,40
14,0	2,88	1,14	0,67	0,13	0,23	10,40
16,0	5,48	1,24	1,28	0,73	0,45	12,22
18,0	7,82	1,10	1,78	1,02	0,53	14,37
19,0	9,13	1,05	2,00	1,19	0,70	15,38
20,0	9,96	1,05	2,27	1,30	0,80	16,38

Note: The mean energy of first neutrons emitted in (n,xnf) reactions for an incident neutron energy of 8.0, 14.0 and 20.0 MeV is 1.08, 1.78 and 3.13 MeV, respectively.

experimental data on secondary neutron spectra for ^{235}U are given. A qualitative comparison of data calculated for ^{235}U with the experimental results of Ref. [6] for a ^{238}U neutron inelastic scattering spectrum for $E = 6$ MeV (see Fig. 1) shows that they agree fairly well.

The mean energy values \bar{E} of the secondary neutrons emitted in the individual reactions are given in the table. Naturally, as the primary neutron energy rises, the secondary neutron spectra become harder. The first neutron emitted has a higher energy, and each subsequent neutron a lower energy. Neutrons emitted in the (n,n') reaction have particularly hard spectrum.

In Figs 3 and 4, the total spectrum and partial spectra of first neutrons from the reactions (n,n'), (n,2n) and (n,3n) are given. The spectrum of pre-fission first neutrons is also given. Their mean energy shows relatively little variation: from 1 to 3 MeV in the 8-20 MeV incident neutron energy region. The shape of these spectra differs from a Maxwellian distribution, especially for high incident neutron energies.

Complete files of evaluated data must include the partial and total fission cross-sections and the secondary neutron spectra for these processes.

Experimental data for ^{238}U show that, where the initial neutron energy is higher than the threshold of the reaction (n,n'f), a significant proportion (about 17%) of the neutrons emitted before fission have a spectrum which differs from a Maxwellian distribution [7]. As a rule, the spectra of prompt fission neutrons given in current files do not allow for this peculiarity. The calculations carried out using the above model permit the spectra of pre-fission neutrons to be obtained.

REFERENCES

- [1] GRUDZEVICH, O.T., IGNATYUK, A.V., MASLOV, V.M. et al., A consistent description of the (n,nf) and (n,xn) reaction cross-sections for transuranium nuclei, In: Neutron Physics (Proc. 6th All-Union Conf. on Neutron Physics, Kiev, 2-6 October 1983) Vol. 2, TsNIiatominform, Moscow (1984) 318-323 [in Russian].

- [2] UHL, M., STROHMAIER, B., Computer code for particle induced activation cross-sections and related topics, Rep. IRK-71/01, Vienna (1976)
- [3] BRAGA-MARCAZZAN, G.M., GADIOLI-ERBA, E., MILAZZO-COLLI, L., SONA, P.G., Analysis of the total (n,p) cross-sections around 14 MeV with the pre-equilibrium exciton model, Phys. Rev. 6 (1972) 1398-1407.
- [4] BLATT, J., WEISKOPF, V., Theoretical nuclear physics, Izd-vo Inostr. Lit., Moscow (1954) [in Russian].
- [5] SEIDEL, K., SEELIGER, D., REIF, R. et al., Pre-equilibrium decay in nuclear reactions, Fiz. Ehlem. Chastits At. Yadra. 7 2 (1976) 499-552 [in Russian].
- [6] KORNILOV, N.V., Cross-sections and spectra of neutrons from the reactions (n,n') and (n,2n) for ^{238}U , Vopr. At. Nauki i Tekhniki: Ser. Yad. Konstanty 4 (1985) 56-60 [in Russian].
- [7] KORNILOV, N.V., Prompt fission neutron spectra for ^{238}U , ibid. 46-50 [in Russian].

SYSTEMATICS OF RADIATION WIDTHS AND LEVEL DENSITY PARAMETERS
IN THE MASS NUMBER RANGE REGION $40 < A < 250$

V.M. Bychkov, O.T. Grudzevich, V.I. Plyaskin

A knowledge of the mean radiation widths of nuclei or, more importantly, of the radiative strength functions is required when calculating, on the basis of a statistical theory, mean radiative capture cross-sections and cross-sections for reactions of the type $(n, \gamma \kappa)$ and $(n, x \gamma)$, and also emission spectra of γ -quanta in various nuclear reactions.

A number of papers dealing with the systematics of mean radiation widths at the neutron binding energy have been published. Fairly detailed information is given in Refs [1-3]. A general disadvantage of these systematics is the complex dependence of the radiation widths on the relative atomic mass of the nucleus, which makes interpolation and prediction of data over a wide range of mass numbers difficult. The present paper suggests a systematics based on a reduced radiative capture strength function for the E1-transition, which eliminates fluctuations in the analysed quantity with neutron binding energy, nuclear level density and γ -quanta energy.

As a result a smooth dependence is obtained for the fitting parameter of the radiative strength function for E1-transitions in relation to the relative atomic mass of the nucleus.

PROCEDURE FOR OBTAINING MEAN RADIATION WIDTH SYSTEMATICS

Basic relationships for mean radiation widths. This paper bases the systematics of mean radiation widths on a determination of the radiative strength function

$$f_{X,L}(\epsilon_{\gamma}) = \frac{\langle \Gamma_{\lambda \gamma \mu}^{X,L} \rangle}{\langle D_{\lambda} \rangle \epsilon_{\gamma}^{2L+1}},$$

where X, L is the type of transition (electrical or magnetic) and its multipolarity;

- ϵ_γ the γ -quanta energy;
 $\langle \Gamma_{\lambda\gamma\mu} \rangle$ the mean radiation width of the transition between the states λ, γ, μ ;
 $\langle D_\lambda \rangle$ the mean distance between resonances;
 λ the compound nucleus resonance system; and
 μ the resonances (levels) at which decay takes place.

The aim of the calculations is to determine the radiative strength function for E1-transitions (f_{E1}) on the basis of existing experimental data on the mean radiation widths and resonance density at the neutron binding energy. It is assumed that the E1-transitions account for the determining contribution to the mean radiative capture width; the contributions of direct and valence captures is disregarded. With those assumptions, the observed mean radiation width can be written as

$$\langle \Gamma_\gamma \rangle_\ell = \langle D \rangle_\ell \sum_J \sum_{I=|J-1|}^{J+1} \int_0^{B_n} f_{E1}(\epsilon_\gamma) \epsilon_\gamma^3 \rho(B_n - \epsilon_\gamma, I) d\epsilon_\gamma, \quad (1)$$

where $\langle \Gamma_\gamma \rangle_\ell$, $\langle D \rangle_\ell$ are the experimental values of the total radiation width and the mean distance between resonances, which are excited by neutrons with an orbital angular momentum ℓ ; B_n is the neutron binding energy in the compound nucleus; $\rho(B_n - \epsilon_\gamma, I)$ is the density of the levels at which decay takes place; I is the total momentum; and J is the total angular momentum. According to the Brink-Axel hypothesis, the function $f_{E1}(\epsilon_\gamma)$ can be written using the inverse photoabsorption cross-section:

$$f_{E1}(\epsilon_\gamma) = C_0 A \epsilon_\gamma \Gamma_R / \left[(\epsilon_\gamma^2 - E_R^2)^2 + \epsilon_\gamma^2 \Gamma_R^2 \right], \quad (2)$$

where C_0 is the desired coefficient, independent of the γ -quanta energy; A is the relative atomic mass of the compound nucleus; and E_R and Γ_R are the Lorentz dependence parameters of the giant dipolar resonance ($E_R = 80 A^{-1/3}$ MeV, $\Gamma_R = 5$ MeV).

The transparency coefficients $T_{E1}(\epsilon_\gamma)$ are related to $f_{E1}(\epsilon_\gamma)$ by the expression $T_{E1}(\epsilon_\gamma) = 2\pi f_{E1}(\epsilon_\gamma)\epsilon_\gamma^3$.

The level density $\rho(U, J)$ must be known in order to establish the systematics of C_0 as a function of the mass number A . The following subsection deals with the systematics of level density parameters, which is used later to calculate the coefficient C_0 using expressions (1) and (2).

Systematics of level density parameters. The Fermi-gas model is widely used in various forms [4-6] to calculate nuclear level densities. In spite of serious defects [7], this model makes it possible to establish simple systematics based on normalization of the energy dependence of the nuclear level density with respect to observed values of $\langle D \rangle_0$ over a fairly wide range of excitation energies. The most widely used level density parameter systematics is that given in Ref. [6] within the framework of a Fermi-gas model with "back-shifting" on the basis of experimental data up to 1973. This systematics is reviewed in the present paper on the basis of contemporary data on neutron resonance density and low-lying level diagrams.

For a level density $\rho(U, J)$, the following relationships [7] are used as functions of the excitation energy U and of the total angular momentum J ;

$$\rho(U, J) = \frac{1}{24\sqrt{2}} \frac{(2J+1)}{6^3 a^{1/4}} \frac{\exp[2\sqrt{a(U-\Delta)} - J(J+1)/2\sigma^2]}{(U-\Delta+t)^{5/4}} ;$$

$$\rho(U) = 2\sigma^2 \rho(U, 0),$$

where a is a level density parameter related to the density of single-particle states in the region of the Fermi-level; Δ is a fitting parameter in the Fermi-gas model with back-shifting; t is the thermodynamic temperature determined by the equation $U - \Delta = at^2 - t$; and σ^2 is the spin dependence parameter.

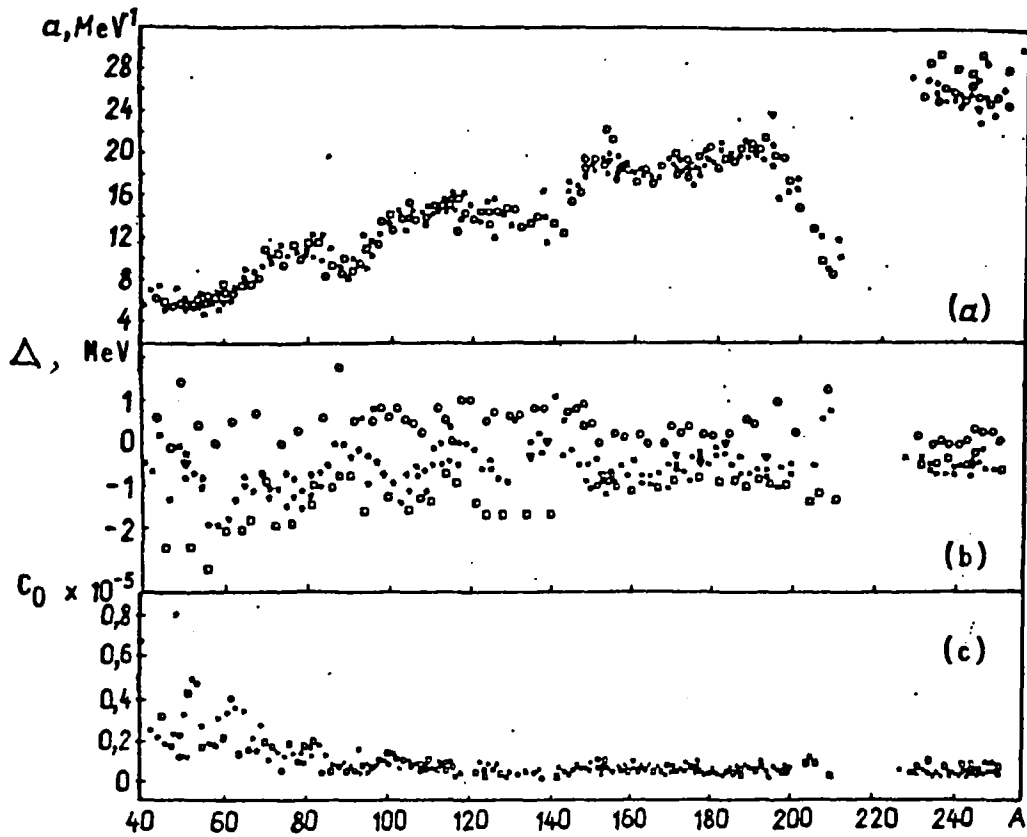


Fig. 1. Level density parameters α (a) and Δ (b) and normalization coefficient radiative strength function C_0 (c) versus mass number A for even-even (O), odd-odd (\square), even-odd (*) and odd-even (∇) nuclei.

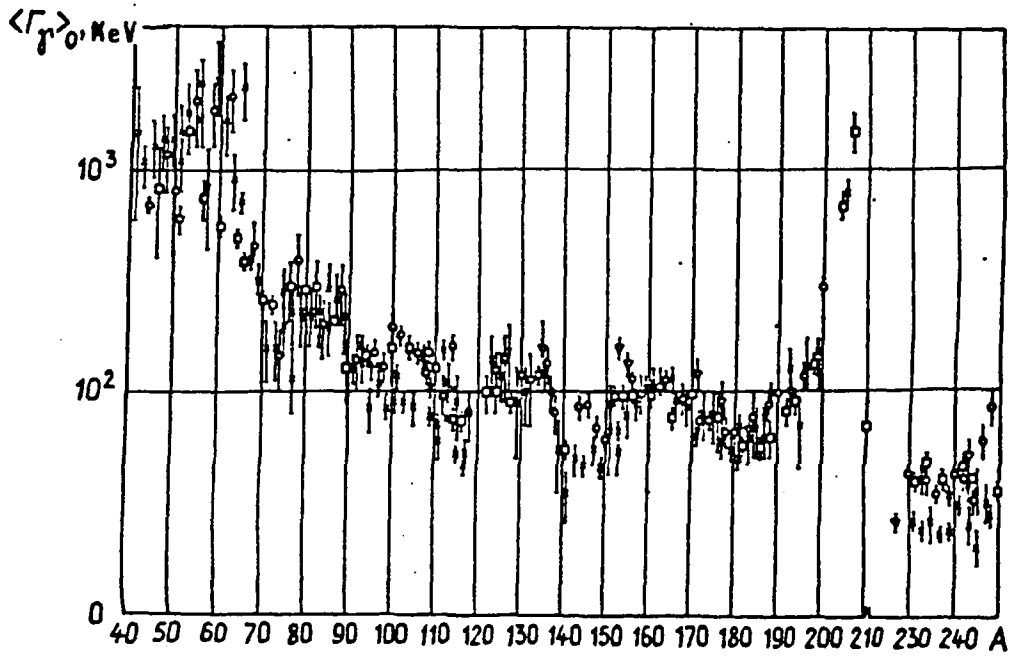


Fig. 2. Experimental values for the mean radiation width $\langle \Gamma_T \rangle_0$ versus mass number A for even-even (O), odd-odd (\square), even-odd (*) and odd-even (∇) nuclei.

The following equations are used to obtain the parameters a and Δ :

$$2/\langle D \rangle_0 = \sum_J \rho(B_n + \Delta E/2, J); \quad (3)$$

$$N_0 = \int_0^{U_0} \rho(U) dU,$$

where N_0 is the number of low-lying levels of the analysed nucleus in the excitation energy range from zero to U_0 .

Experimental values of $\langle D \rangle_0$ were taken from Ref. [2] and given in the table. Values of N_0 and U_0 were determined from graphs of the energy dependence of the number of lower levels of the nucleus. The level diagrams were taken from Ref. [8].

The values obtained for the parameters a and Δ are shown in the table and in Fig. 1. Shell effects are clearly visible in the behaviour of parameter a in relation to relative atomic mass. With this approach, these effects cannot be taken into account with sufficient accuracy even by introducing (as suggested in Ref. [9]) a dependence of a on the excitation energy and a shell correction. Shell and collective effects, together with pairing effects, combine in a complex manner in the behaviour of the parameter Δ in relation to relative atomic mass. The systematics of the parameter Δ are very problematic in this model.

Mean radiation width systematics. We obtained the coefficient C_0 with the help of Eqs (1) and (2) using experimental values of $\langle D \rangle_0$ and $\langle \Gamma_\gamma \rangle_0$ from Ref. [2] and level density parameters based on the above systematics. It should be noted that in some cases, particularly for medium and light nuclei, the experimental values of $\langle \Gamma_\gamma \rangle_0$ and $\langle D \rangle_0$ are unreliable owing to statistical problems. Indirect data on the ratio $\langle \Gamma_\gamma \rangle_0 / \langle D \rangle_0$ obtained from analysis of neutron radiative capture cross-sections in the unresolved resonance range, in particular at a neutron energy of 30 keV [10], were therefore also considered.

Level density parameters α and Δ normalization coefficient of the radiative strength function C_0 .

Compound nucleus	B_n , MeV	$\langle D \rangle_0$, eV	$\langle \Gamma_J \rangle_0$, MeV	α , MeV ⁻¹	Δ , MeV	$2C_0 \times 10^5$, MeV ⁻¹
				$J = J_{TB}$		
41 20 Ca	8,363	45000,0	1500,0	5,16	-0,46	1,36
43 20 Ca	7,933	8600,0	1100,0	6,95	-0,65	2,00
44 20 Ca	11,132	1500,0	700,0	6,20	0,63	0,50
45 20 Ca	7,415	16000,0	1300,0	7,39	0,20	3,60
46 21 Sc	8,760	1300,0	840,0	5,94	-2,55	0,44
47 22 Ti	8,880	20000,0	1400,0	5,52	-1,27	0,63
48 22 Ti	11,628	2200,0	1200,0	5,50	0,13	0,38
49 22 Ti	8,142	13000,0	1400,0	7,04	-0,12	1,72
50 22 Ti	10,945	5000,0	810,0	5,67	1,36	0,46
51 22 Ti	6,372	125000,0	1100,0	5,91	-0,21	1,39
51 23 V	11,051	2700,0	600,0	5,55	0,49	0,23
52 23 V	7,311	4400,0	1500,0	5,72	-2,54	0,85
51 24 Cr	9,261	15000,0	1500,0	5,84	-0,80	0,65
53 24 Cr	7,940	45000,0	1850,0	5,65	-0,70	1,00
54 24 Cr	9,719	7100,0	2100,0	5,85	0,43	0,95
55 24 Cr	6,246	60000,0	2500,0	6,42	-0,77	3,19
56 25 Mn	7,270	2700,0	750,0	5,88	-3,27	0,32
55 26 Fe	9,299	20000,0	1800,0	5,50	-1,03	0,55
57 26 Fe	7,646	25000,0	850,0	5,70	-1,85	0,39
58 26 Fe	10,044	6500,0	1000,0	6,07	0,05	0,36
59 26 Fe	6,581	24000,0	3000,0	6,39	-1,86	2,37
60 27 Co	7,492	1100,0	560,0	7,30	-1,94	0,40
59 28 Ni	9,000	16700,0	2600,0	5,48	-1,81	0,63
61 28 Ni	7,820	16000,0	1700,0	6,30	-1,74	0,71
62 28 Ni	10,598	1800,0	2200,0	6,82	0,51	0,86
63 28 Ni	6,839	19100,0	910,0	6,82	-1,35	0,74
65 28 Ni	6,098	19900,0	2400,0	7,85	-0,80	3,93
64 29 Cu	7,916	1040,0	490,0	7,47	-1,98	0,25
66 29 Cu	7,067	1470,0	385,0	7,92	-1,78	0,28
65 30 Zn	7,980	2008,0	726,0	8,91	-0,93	0,67
67 30 Zn	7,053	4700,0	400,0	8,65	-1,13	0,40
68 30 Zn	10,198	510,0	460,0	8,24	0,72	0,28

(cont.)

Compound nucleus	B_n , MeV	$\langle D \rangle_0$, eV	$\langle \Gamma_f \rangle_0$, MeV	α , MeV ⁻¹	Δ , MeV	$2C_0 \times 10^5$, MeV ⁻¹
				$\alpha = \Delta_{TB}$		
⁶⁹ ₃₀ Zn	6,482	5770,0	320,0	9,31	-0,69	0,56
⁷¹ ₃₀ Zn	5,835	6900,0	-	9,58	-1,05	-
⁷⁰ ₃₁ Ga	7,655	181,0	262,0	10,62	-0,92	0,36
⁷² ₃₁ Ga	6,521	225,0	237,0	10,38	-2,04	0,31
⁷¹ ₃₂ Ge	7,416	930,0	165,0	10,18	-1,23	0,19
⁷³ ₃₂ Ge	6,782	960,0	162,0	11,01	-1,11	0,27
⁷⁴ ₃₂ Ge	10,200	82,0	145,0	9,42	-0,02	0,09
⁷⁵ ₃₂ Ge	6,506	3000,0	195,0	10,38	-0,71	0,32
⁷⁷ ₃₂ Ge	6,072	3750,0	115,0	10,59	-0,76	0,22
⁷⁶ ₃₃ As	7,328	75,0	300,0	11,08	-1,88	0,33
⁷⁵ ₃₄ Se	8,028	420,0	280,0	10,31	-1,45	0,23
⁷⁷ ₃₄ Se	7,418	667,0	230,0	10,65	-1,23	0,25
⁷⁸ ₃₄ Se	10,497	146,0	300,0	10,07	0,26	0,17
⁷⁹ ₃₄ Se	6,961	1390,0	230,0	10,43	-1,09	0,26
⁸¹ ₃₄ Se	6,701	2000,0	230,0	10,19	-1,18	0,25
⁸³ ₃₄ Se	5,896	6700,0	-	9,82	-1,00	-
⁸⁰ ₃₅ Br	7,892	47,0	293,0	11,67	-1,37	0,31
⁸² ₃₅ Br	7,593	94,0	300,0	11,62	-0,99	0,36
⁷⁹ ₃₆ Kr	8,360	230,0	230,0	10,73	-1,46	0,17
⁸¹ ₃₆ Kr	7,882	200,0	230,0	12,25	-0,75	0,32
⁸³ ₃₆ Kr	7,465	382,0	230,0	12,10	-0,64	0,34
⁸⁴ ₃₆ Kr	10,519	326,0	200,0	8,33	0,57	0,07
⁸⁶ ₃₇ Rb	8,650	200,0	205,0	9,28	-1,05	0,09
⁸⁸ ₃₇ Rb	6,078	1760,0	-	9,94	-0,82	-
⁸⁵ ₃₈ Sr	8,524	383,0	290,0	11,05	-0,48	0,24
⁸⁷ ₃₈ Sr	8,428	3000,0	260,0	9,13	-0,09	0,14
⁸⁸ ₃₈ Sr	11,113	380,0	290,0	8,65	1,76	0,12
⁸⁹ ₃₈ Sr	6,364	62000,0	220,0	7,51	0,02	0,14
⁹⁰ ₃₉ Y	6,857	4000,0	130,0	8,92	-0,74	0,08
⁹¹ ₄₀ Zr	7,193	8600,0	130,0	9,67	0,34	0,12
⁹² ₄₀ Zr	8,639	640,0	140,0	9,51	0,54	0,09
⁹³ ₄₀ Zr	6,732	3100,0	135,0	12,17	0,56	0,29

(cont.)

Compound nucleus	B_n , MeV	$\langle D \rangle_0$, eV	$\langle \Gamma_g \rangle_0$, MeV	α , MeV ⁻¹	Δ , MeV	$2C_D \times 10^5$, MeV ⁻¹
				$J = J_{TB}$		
⁹⁵ Zr ₄₀	6,470	3800,0	85,0	10,21	-0,89	0,07
⁹⁷ Zr ₄₀	5,572	5200,0	130,0	14,39	0,83	0,75
⁹⁴ Nb ₄₁	7,229	90,0	145,0	10,81	-1,61	0,11
⁹³ Mo ₄₂	8,067	3600,0	160,0	9,30	-0,14	0,08
⁹⁵ Mo ₄₂	7,371	1150,0	135,0	11,40	-0,30	0,14
⁹⁶ Mo ₄₂	9,154	91,0	150,0	11,36	0,53	0,12
⁹⁷ Mo ₄₂	6,821	950,0	100,0	12,29	-0,41	0,14
⁹⁸ Mo ₄₂	8,642	42,0	130,0	13,27	0,66	0,18
⁹⁹ Mo ₄₂	5,926	970,0	85,0	13,28	-0,69	0,18
¹⁰¹ Mo ₄₂	5,398	700,0	90,0	14,48	-0,91	0,25
¹⁰⁰ Tc ₄₃	6,764	17,6	160,0	14,08	-1,25	0,26
¹⁰⁰ Ru ₄₄	9,637	25,0	195,0	12,54	0,59	0,16
¹⁰² Ru ₄₄	9,220	18,0	180,0	13,68	0,68	0,20
¹⁰³ Ru ₄₄	6,232	550,0	90,0	12,62	-1,38	0,10
¹⁰⁴ Ru ₄₄	8,905	7,5	-	15,21	0,54	-
¹⁰⁵ Ru ₄₄	5,910	300,0	85,0	14,52	-1,09	0,17
¹⁰⁴ Rh ₄₅	7,000	34,0	160,0	14,21	-1,54	0,18
¹⁰⁵ Pd ₄₆	7,094	153,0	-	14,17	-0,69	-
¹⁰⁶ Pd ₄₆	9,562	10,3	150,0	13,67	0,44	0,13
¹⁰⁷ Pd ₄₆	6,530	270,0	-	14,09	-0,82	-
¹⁰⁸ Pd ₄₆	9,223	11,4	125,0	13,77	0,25	0,11
¹⁰⁹ Pd ₄₆	6,154	200,0	77,0	14,81	-1,10	0,14
¹¹¹ Pd ₄₆	5,760	450,0	60,0	16,93	0,10	0,26
¹⁰⁸ Ag ₄₇	7,267	22,0	140,0	15,21	-1,08	0,19
¹¹⁰ Ag ₄₇	6,806	18,7	130,0	16,13	-1,14	0,22
¹⁰⁷ Cd ₄₈	7,927	135,0	155,0	13,24	-0,64	0,14
¹⁰⁹ Cd ₄₈	7,360	120,0	105,0	14,35	-0,59	0,13
¹¹¹ Cd ₄₈	6,977	155,0	71,0	14,75	-0,52	0,11
¹¹² Cd ₄₈	9,395	20,0	96,0	14,98	0,80	0,10
¹¹³ Cd ₄₈	6,544	190,0	77,0	15,30	-0,50	0,14
¹¹⁴ Cd ₄₈	9,041	21,0	160,0	14,96	0,46	0,17
¹¹⁵ Cd ₄₈	6,145	235,0	54,0	16,00	-0,41	0,13

(cont.)

Compound nucleus	B_n , MeV	$\langle D \rangle_0$, eV	$\langle \Gamma_g \rangle_0$, MeV	α , MeV ⁻¹	Δ , MeV	$2C_0 \times 10^5$, MeV ⁻¹
				$J = J_{TB}$		
¹¹⁷ ₄₈ Ca	5,770	390,0	47,0	15,84	-0,47	0,12
¹¹⁴ ₄₉ In	7,275	9,0	75,0	15,29	-0,68	0,11
¹¹⁶ ₄₉ In	6,784	9,4	77,0	15,66	-0,93	0,13
¹¹³ ₅₀ Sn	7,746	157,0	110,0	14,36	0,01	0,14
¹¹⁵ ₅₀ Sn	7,546	283,0	90,0	14,52	0,40	0,13
¹¹⁶ ₅₀ Sn	9,562	50,0	0,0	12,45	-0,02	-
¹¹⁷ ₅₀ Sn	6,944	629,0	52,0	13,58	-0,04	0,07
¹¹⁸ ₅₀ Sn	9,326	50,0	80,0	14,26	1,07	0,07
¹¹⁹ ₅₀ Sn	6,484	478,0	0,0	14,92	-0,03	-
¹²⁰ ₅₀ Sn	9,106	90,0	-	13,65	0,98	-
¹²¹ ₅₀ Sn	6,172	1640,0	-	13,36	-0,13	-
¹²⁵ ₅₀ Sn	5,733	2500,0	-	13,28	-0,27	-
¹²² ₅₁ Sb	6,806	18,0	100,0	14,44	-1,39	0,09
¹²⁴ ₅₁ Sb	6,467	38,0	100,0	13,12	-1,72	0,07
¹²³ ₅₂ Te	6,933	132,0	140,0	15,17	-0,56	0,18
¹²⁴ ₅₂ Te	9,424	25,0	124,0	14,31	0,52	0,09
¹²⁵ ₅₂ Te	6,572	147,0	120,0	15,57	-0,63	0,17
¹²⁶ ₅₂ Te	9,120	48,0	142,0	14,12	0,69	0,11
¹²⁷ ₅₂ Te	6,290	470,0	149,0	13,97	-0,80	0,16
¹²⁹ ₅₂ Te	6,086	992,0	87,0	13,06	-0,88	0,08
¹³¹ ₅₂ Te	5,925	870,0	-	16,54	0,48	-
¹²⁸ ₅₃ I	6,826	14,5	90,0	14,29	-1,69	0,07
¹³⁰ ₅₄ Xe	9,255	32,0	121,0	14,46	0,62	0,08
¹³² ₅₄ Xe	8,936	74,0	114,0	12,87	0,64	0,06
¹³⁴ ₅₅ Cs	6,691	22,7	120,0	13,29	-1,72	0,07
¹³⁵ ₅₅ Cs	8,828	27,0	160,0	12,32	-0,31	0,06
¹³⁵ ₅₆ Ba	6,794	230,0	120,0	15,64	-0,06	0,16
¹³⁶ ₅₆ Ba	9,107	40,0	135,0	13,83	0,84	0,08
¹³⁷ ₅₆ Ba	6,898	920,0	100,0	13,81	0,23	0,10
¹³⁸ ₅₆ Ba	8,611	380,0	80,0	11,38	0,81	0,03
¹³⁹ ₅₇ La	8,778	23,0	-	13,12	-	-
¹⁴⁰ ₅₇ La	5,161	283,0	55,0	13,18	-1,73	0,05

(cont.)

Compound nucleus	B_n, MeV	$\langle D \rangle_0, \text{eV}$	$\langle \Gamma_f \rangle_0, \text{MeV}$	α, MeV^{-1}	Δ, MeV	$2C_0 \times 10^5, \text{MeV}^{-1}$
				$\mathcal{J} = \mathcal{J}_{TB}$		
$^{137}_{58}\text{Ce}$	7,490	50,0	-	16,44	-0,22	-
$^{141}_{58}\text{Ce}$	5,428	3200,0	35,0	17,39	1,10	0,17
$^{143}_{58}\text{Ce}$	5,146	1000,0	-	16,44	-0,29	-
$^{143}_{60}\text{Nd}$	6,123	663,0	50,0	16,92	0,55	0,12
$^{144}_{60}\text{Nd}$	7,817	36,5	86,0	15,24	0,74	0,09
$^{145}_{60}\text{Nd}$	5,756	432,0	47,0	16,67	-0,22	0,09
$^{146}_{60}\text{Nd}$	7,565	17,0	87,0	16,12	0,31	0,10
$^{147}_{60}\text{Nd}$	5,292	290,0	55,0	17,76	-0,55	0,13
$^{148}_{60}\text{Nd}$	7,334	5,0	-	19,30	0,39	-
$^{149}_{60}\text{Nd}$	5,039	167,0	46,0	18,62	-0,90	0,11
$^{151}_{60}\text{Nd}$	5,334	164,0	67,0	19,25	-0,40	0,19
$^{148}_{62}\text{Sm}$	8,140	4,7	69,0	18,25	0,86	0,10
$^{149}_{62}\text{Sm}$	5,873	90,0	-	18,62	-0,49	-
$^{150}_{62}\text{Sm}$	7,986	1,9	62,0	19,25	0,46	0,09
$^{151}_{62}\text{Sm}$	5,592	49,0	87,0	19,13	-1,04	0,17
$^{152}_{62}\text{Sm}$	8,269	1,0	95,0	18,75	0,03	0,11
$^{153}_{62}\text{Sm}$	5,867	46,0	67,0	18,10	-1,21	0,10
$^{155}_{62}\text{Sm}$	5,814	115,0	79,0	17,82	-0,70	0,13
$^{204}_{81}\text{Tl}$	6,655	360,0	690,0	12,66	-1,29	0,14
$^{206}_{81}\text{Tl}$	6,503	5500,0	1500,0	9,44	-1,19	0,14
$^{205}_{82}\text{Pb}$	6,734	1520,0	770,0	12,21	-0,47	0,24
$^{207}_{82}\text{Pb}$	6,740	42500,0	-	9,01	0,58	-
$^{208}_{82}\text{Pb}$	7,368	36000,0	-	8,49	1,26	-
$^{209}_{82}\text{Pb}$	3,938	105000,0	-	11,67	0,75	-
$^{210}_{83}\text{Bi}$	4,591	4500,0	70,0	10,15	-1,33	0,02
$^{152}_{63}\text{Eu}$	6,336	0,7	92,0	21,91	-1,00	0,21
$^{153}_{63}\text{Eu}$	8,526	0,3	160,0	19,00	-0,79	0,13
$^{154}_{63}\text{Eu}$	6,444	1,1	95,0	21,05	-0,90	0,18
$^{155}_{63}\text{Eu}$	8,174	0,9	135,0	17,82	-0,69	0,10
$^{156}_{63}\text{Eu}$	6,325	4,8	96,0	18,46	-1,03	0,13
$^{153}_{64}\text{Gd}$	6,464	15,0	54,0	19,25	-0,94	0,08
$^{155}_{64}\text{Gd}$	6,442	14,5	88,0	19,44	-0,94	0,13

(cont.)

Compound nucleus	B_n, MeV	$\langle D \rangle_0, \text{eV}$	$\langle \Gamma_f \rangle_0, \text{MeV}$	$J = J_{TB}$		$2C_0 \times 10^5, \text{MeV}^{-1}$
				α, MeV^{-1}	Δ, MeV	
$^{156}_{64}\text{Gd}$	8,535	1,8	108,0	18,52	0,17	0,10
$^{157}_{64}\text{Gd}$	6,360	36,0	88,0	18,84	-0,63	0,13
$^{158}_{64}\text{Gd}$	7,937	4,9	97,0	18,10	0,15	0,10
$^{159}_{64}\text{Gd}$	5,994	85,0	105,0	17,89	-0,75	0,15
$^{161}_{64}\text{Gd}$	5,633	202,0	111,0	17,98	-0,45	0,19
$^{160}_{65}\text{Tb}$	6,382	4,4	97,0	18,53	-1,30	0,11
$^{161}_{66}\text{Dy}$	6,451	27,3	108,0	17,98	-1,12	0,11
$^{162}_{66}\text{Dy}$	8,195	2,7	110,0	18,09	0,18	0,10
$^{163}_{66}\text{Dy}$	6,272	64,6	112,0	17,73	-0,77	0,13
$^{164}_{66}\text{Dy}$	7,655	6,8	113,0	17,15	-0,07	0,10
$^{165}_{66}\text{Dy}$	5,715	147,0	114,0	17,46	-0,83	0,15
$^{166}_{67}\text{Ho}$	6,243	4,6	77,0	18,40	-1,03	0,09
$^{163}_{68}\text{Er}$	6,907	7,0	-	19,70	-0,95	-
$^{165}_{68}\text{Er}$	6,650	23,0	-	18,29	-0,94	-
$^{167}_{68}\text{Er}$	6,436	38,0	92,0	18,58	-0,66	0,11
$^{168}_{68}\text{Er}$	7,771	4,6	92,0	17,57	0,09	0,08
$^{169}_{68}\text{Er}$	6,003	100,0	85,0	17,04	-1,03	0,08
$^{171}_{68}\text{Er}$	5,681	125,0	-	18,81	-0,47	-
$^{170}_{69}\text{Tm}$	6,594	7,3	97,0	19,41	-0,88	0,11
$^{171}_{69}\text{Tm}$	7,490	3,7	122,0	19,17	-0,30	0,12
$^{169}_{70}\text{Yb}$	6,867	22,8	-	18,73	-0,54	-
$^{170}_{70}\text{Yb}$	8,469	2,2	-	17,92	0,36	-
$^{171}_{70}\text{Yb}$	6,617	37,0	63,0	18,45	-0,57	0,07
$^{172}_{70}\text{Yb}$	8,020	5,8	75,0	19,06	0,23	0,07
$^{173}_{70}\text{Yb}$	6,367	70,0	80,0	17,73	-0,65	0,08
$^{174}_{70}\text{Yb}$	7,465	7,8	74,0	18,49	0,40	0,08
$^{175}_{70}\text{Yb}$	5,822	162,0	80,0	18,45	-0,31	0,12
$^{177}_{70}\text{Yb}$	5,566	185,0	82,0	19,17	-0,22	0,15
$^{176}_{71}\text{Lu}$	6,293	3,6	77,0	19,43	-0,78	0,10
$^{177}_{71}\text{Lu}$	7,072	1,7	90,0	19,17	-0,45	0,10
$^{175}_{72}\text{Hf}$	6,708	27,0	-	18,23	-0,64	-
$^{177}_{72}\text{Hf}$	6,380	32,0	60,0	19,99	-0,32	0,09

(cont.)

Compound nucleus	E_n , MeV	$\langle D \rangle_0$, eV	$\langle \Gamma \rangle_0$, MeV	α , MeV ⁻¹	Δ , MeV	$2C_0 \times 10^5$, MeV ⁻¹
				$J = J_{TB}$		
¹⁷⁸ ₇₂ Hf	7,265	2,4	66,0	20,17	0,19	0,09
¹⁷⁹ ₇₂ Hf	6,099	62,0	54,0	19,09	-0,47	0,07
¹⁸⁰ ₇₂ Hf	7,387	4,4	66,0	18,52	0,17	0,07
¹⁸¹ ₇₂ Hf	5,694	94,0	50,0	20,51	-0,11	0,11
¹⁸² ₇₃ Ta	6,063	4,4	58,0	19,56	-0,86	0,07
¹⁸³ ₇₃ Ta	6,928	4,7	67,0	19,67	0,03	0,08
¹⁸¹ ₇₄ W	6,686	23,0	70,0	20,06	-0,24	0,09
¹⁸³ ₇₄ W	6,191	66,0	62,0	19,52	-0,20	0,09
¹⁸⁴ ₇₄ W	7,411	13,0	77,0	19,24	0,25	0,08
¹⁸⁵ ₇₄ W	5,749	81,0	69,0	19,58	-0,48	0,10
¹⁸⁷ ₇₄ W	5,466	90,0	61,0	20,80	-0,30	0,13
¹⁸⁶ ₇₅ Re	6,179	3,1	57,0	20,30	-0,84	0,07
¹⁸⁸ ₇₅ Re	5,873	4,0	61,0	20,37	-0,96	0,08
¹⁸⁷ ₇₆ Os	6,297	26,0	77,0	19,63	-0,73	0,08
¹⁸⁸ ₇₆ Os	7,989	4,4	88,0	20,52	0,56	0,09
¹⁸⁹ ₇₆ Os	5,923	38,0	100,0	20,00	-0,68	0,13
¹⁹⁰ ₇₆ Os	7,793	3,4	101,0	20,27	0,52	0,11
¹⁹¹ ₇₆ Os	5,761	70,0	-	19,50	-0,63	-
¹⁹³ ₇₆ Os	5,635	115,0	-	18,82	-0,67	-
¹⁹² ₇₇ Ir	6,197	3,0	81,0	21,28	-0,79	0,11
¹⁹³ ₇₇ Ir	7,817	0,6	100,0	23,64	-0,29	0,12
¹⁹⁴ ₇₇ Ir	6,066	7,0	93,0	19,72	-0,95	0,09
¹⁹³ ₇₈ Pt	6,247	12,0	130,0	20,91	-0,84	0,15
¹⁹⁵ ₇₈ Pt	6,109	240,0	70,0	15,76	-0,95	0,04
¹⁹⁶ ₇₈ Pt	7,920	18,0	120,0	19,60	1,08	0,12
¹⁹⁷ ₇₈ Pt	5,850	380,0	130,0	18,42	-0,55	0,10
¹⁹⁹ ₇₈ Pt	5,571	340,0	125,0	17,58	-0,46	0,13
¹⁹⁸ ₇₉ Au	6,512	16,5	128,0	17,16	-0,93	0,08
¹⁹⁹ ₈₀ Hg	6,648	105,0	150,0	16,67	-0,67	0,08
²⁰⁰ ₈₀ Hg	8,028	100,0	295,0	14,92	0,32	0,10
²²⁷ ₈₈ Ra	4,565	30,0	26,0	27,33	-0,33	0,11
²³⁰ ₉₀ Th	6,780	0,5	43,0	25,49	0,18	0,07

(cont.)

Compound nucleus	B_n , MeV	$\langle D \rangle_0$, eV	$\langle r_g \rangle_0$, MeV	α , MeV ⁻¹	Δ , MeV	$2C_0 \times 10^5$, MeV ⁻¹
				$J = J_{TB}$		
²³¹ ₉₀ Th	5,129	9,6	26,0	27,24	-0,39	0,07
²³³ ₉₀ Th	4,786	16,8	24,0	26,79	-0,54	0,07
²³² ₉₁ Pa	5,562	0,4	40,0	28,71	-0,53	0,10
²³⁴ ₉₁ Pa	5,197	0,7	47,0	29,44	-0,52	0,15
²³³ ₉₂ U	5,743	4,6	40,0	25,92	-0,50	0,07
²³⁴ ₉₂ U	6,840	0,6	40,0	24,86	0,06	0,05
²³⁵ ₉₂ U	5,297	10,6	26,0	24,87	-0,75	0,04
²³⁶ ₉₂ U	6,545	0,4	35,0	26,06	0,10	0,06
²³⁷ ₉₂ U	5,124	15,0	23,0	25,08	-0,67	0,04
²³⁸ ₉₂ U	6,143	3,5	-	25,78	0,09	-
²³⁹ ₉₂ U	4,807	21,7	23,6	25,69	-0,64	0,05
²³⁸ ₉₃ Np	5,487	0,6	40,0	28,16	-0,42	0,10
²³⁹ ₉₄ Pu	5,656	9,0	34,4	24,70	-0,56	0,05
²⁴⁰ ₉₄ Pu	6,534	2,2	43,3	24,90	-0,04	0,06
²⁴¹ ₉₄ Pu	5,240	12,4	30,7	25,71	-0,52	0,06
²⁴² ₉₄ Pu	6,309	0,7	40,8	26,52	0,12	0,08
²⁴³ ₉₄ Pu	5,037	13,3	25,4	27,13	-0,36	0,07
²⁴⁵ ₉₄ Pu	4,720	17,0	20,0	28,79	-0,21	0,08
²⁴² ₉₅ Am	5,528	0,6	46,0	27,63	-0,51	0,10
²⁴³ ₉₅ Am	6,377	0,4	50,0	24,40	-0,41	0,06
²⁴⁴ ₉₅ Am	5,363	0,6	39,0	29,28	-0,25	0,12
²⁴³ ₉₆ Cm	5,701	12,8	38,0	23,08	-0,75	0,04
²⁴⁴ ₉₆ Cm	6,799	0,8	33,0	25,31	0,35	0,05
²⁴⁵ ₉₆ Cm	5,519	11,8	36,0	25,21	-0,40	0,06
²⁴⁶ ₉₆ Cm	6,451	1,4	60,0	24,91	0,34	0,09
²⁴⁷ ₉₆ Cm	5,175	30,0	32,0	23,88	-0,56	0,05
²⁴⁸ ₉₆ Cm	6,210	1,4	85,0	25,42	0,34	0,15
²⁴⁹ ₉₆ Cm	4,713	25,0	28,0	26,14	-0,58	0,07
²⁵⁰ ₉₇ Bk	4,969	1,0	36,0	27,92	-0,61	0,09
²⁵⁰ ₉₈ Cf	6,619	0,7	40,0	24,58	0,11	-
²⁵³ ₉₈ Cf	4,793	27,0	-	30,15	0,30	-

The values obtained for C_0 are shown in the table and in Fig. 1. For nuclei with $A > 80$, the values of C_0 (in MeV^{-1}) is described well by the relationship $C_0 = 10^{-3} A^{-3/2}$. Values of $\langle \Gamma_\gamma \rangle_0$ as a function of the mass number of the nucleus are plotted in Fig. 2.

RECOMMENDATIONS CONCERNING THE USE OF THE SYSTEMATICS OBTAINED FOR RADIATION WIDTHS AND LEVEL DENSITY PARAMETERS

The parameters in the table are particularly recommended for calculations using a statistical theory of nuclear reactions. For nuclei not included in the table for lack of experimental data, it is recommended to approximate the coefficient C_0 by the function $C_0 = 10^{-3} A^{-3/2}$; the parameter a can be found by interpolation of data for neighbouring nuclei (see Fig. 1), and the parameter Δ can be determined by considering the following: for most of the nuclei for which data on the neutron resonance density are not available, experimental data do exist concerning the lower levels. Therefore the values of N_0 and U_0 for the nucleus in question can be determined, and then, using the parameter a found from the systematics, the parameter Δ can be determined by solving Eq. (3).

REFERENCES

- [1] ZAKHAROVA, S.M., STAVINSKIJ, V.S., SHUBIN Yu.N., *Yad. Konst.*, 7 (1971) Appendix 2.
- [2] BELANOVA, T.S., IGNATYUK, A.V., PASHCHENKO, A.B., PLYASKIN, V.I., *Neutron Radiative Capture*, Ehnergoatomizdat, Moscow (1986).
- [3] ALLEN, B.J., BERGQVIST, I., CHRIEN, R.E., et al., *Neutron radioactive capture*, Pergamon Press (1984).
- [4] GILBERT, A., CAMERON, A., *Can. J. Phys.*, 43 (1965) 1446.
- [5] VONACH, H.K., HUIZENGA, J.R., *Phys. Rev.*, B138 (1965) 1372.
- [6] DILG, W., SCHANTL, W., VONACH, H., UHL, M., *Nucl. Phys.*, A217 (1973) 269.
- [7] IGNATYUK, A.V., *Statistical Properties of Excited Atomic Nuclei*, Ehnergoatomizdat, Moscow (1983) [in Russian].

- [8] LEDERER, C.M., SHIRLEY, V.S., Table of isotopes, 7th Ed., New York (1978).
- [9] IGNATYUK, A.V., SMIRENKIN, G.N., TISHIN, A.S., Yad. Fiz., 21 (1975) 485.
- [10] BELANOVA, T.S., GORBACHEVA, L.V., GRUDZEVICH, O.T., et al., At. Ehnerg., 57 (1984) 243.

INTEGRAL CROSS-SECTIONS FOR THE REACTIONS

$^{51}\text{V}(n,\alpha)^{48}\text{Sc}$, $^{93}\text{Nb}(n,2n)^{92}\text{Nb}^m$ and $^{90}\text{Zr}(n,2n)^{89}\text{Zr}$

E.I. Grigor'ev, Yu.A. Melekhin, V.P. Yaryna

The reactions $^{51}\text{V}(n,\alpha)^{48}\text{Sc}$, $^{93}\text{Nb}(n,2n)^{92}\text{Nb}^m$ and $^{90}\text{Zr}(n,2n)^{89}\text{Zr}$ are of practical interest for neutron activation spectrometry of reactor neutron fields at energies higher than 10 MeV because the reaction products have convenient decay characteristics, there are extensive experimental data on the cross-sections, and materials with the necessary purity are available for making detectors. However, there are no recommended integral cross-section values (e.g. the mean cross-sections for ^{235}U and ^{252}Cf fission neutrons) for the selection of suitable evaluated data on the energy dependencies of the cross-sections for these reactions.

The authors of this paper determined the mean reaction cross-sections for neutrons in the ^{235}U fission spectrum, evaluated these cross-sections on the strength of all the published data, and compared them with the calculated integral cross-sections from different libraries.

The mean reaction cross-sections for ^{235}U fission neutrons (σ^U) were determined experimentally in water-water reactor fields using the method in Ref. [1]. The experimental results are not based on any "standard" (mean cross-section of a reference reaction in relation to which the unknown cross-section is determined). However, for the purposes of comparison with data in the literature, the mean cross-sections for the reactions $^{58}\text{Ni}(n,p)^{58}\text{Co}$ and $^{27}\text{Al}(n,\alpha)^{24}\text{Na}$ were determined for the experimental conditions, their values being 104 and 0.69 mb, respectively. The samples studied were disks with a diameter of 10 mm and a mass of 200-300 mg. Vanadium and zirconium in metallic form and extremely pure niobium pentoxide were used. The samples were irradiated in cadmium screens. The activity was measured by the γ -spectrometric method. Table 1 presents the measurement results and compares them with data in the literature. The decay characteristics of the reaction products are shown in Table 2.

In order to obtain the evaluated values, the authors' data were renormalized to the following "standards": (S) - 62.8 mb, (Ni) - 103 mb, (Fe) - 78.7 mb and (Al) - 0.685 mb. The evaluated mean cross-sections for vanadium and niobium were obtained as weighted means for the set of renormalized values. The error in the evaluated results represents a mean square deviation for the set considered. The results available for zirconium are insufficient to enable a correct evaluation to be made and therefore the result obtained in this experiment is given as a recommended value for further application.

The existing experimental data on the mean reaction cross-sections in the ^{252}Cf fission neutron spectrum are contained in only two works, and analysis of the data shows that the results in Ref. [9] are systematically 20-30% higher than the data in Ref. [10]. Table 3 shows data on the mean cross-sections for three reactions in the ^{252}Cf spectrum and the results of converting these values to cross-sections in the ^{235}U spectrum. The description of the ^{235}U spectrum in the BKS-2 library [11] was used for the calculation.

Examination of some of the evaluations of the pattern of reaction cross-sections enables us to give a preference to the cross-sections from the BOSPOR library [12]. Table 4 shows the results of calculating the mean

Table 1. Mean cross-sections for reactions in the ^{235}U spectrum, mb

$^{51}\text{V}(n, \alpha)^{48}\text{Sc}$				$^{93}\text{Nb}(n, 2n)^{92}\text{Nb}$				$^{90}\text{Zr}(n, 2n)^{89}\text{Zr}$			
Ref.	Results given there	Authors' standard	Normalized value	Ref.	Results given there	Authors' standard	Normalized value	Ref.	Results given there	Authors' standard	Normalized value
[2]	0,028	(S)60	0,029	[4]	$0,402 \pm 0,034$	(Ni)104	0,418	[2]	0,03	(S)60	0,031
[3]	$0,0153 \pm 0,0027$	(Fe)67	0,0180	[5]	$0,430 \pm 0,028$	{(Al)0,63; (Ni)102}	- 0,434	[8]	$0,0687 \pm 0,0100$	(Fe)72,6	0,074
[4]	$0,0217 \pm 0,0015$	{(Ni)104; (Al)0,63}	0,0225	[6]	$0,475 \pm 0,032$	{(Ni)108,5; (Al)0,705}	0,456	[5]	$0,229 \pm 0,015$	(Ni)102	0,231
[5]	$0,0197 \pm 0,0012$	(Ni)102	0,0199	[3]	$0,370 \pm 0,030$	(Fe)67	0,435	[6]	$0,247 \pm 0,017$	{(Ni)108,5; (Al)0,705}	0,237; -
Present work	$0,0215 \pm 0,0008$	-	0,0215	[7]	$0,420 \pm 0,007$	-	0,420	Present work	$0,096 \pm 0,008$	-	0,096
				Present work	$0,416 \pm 0,015$	-	0,416				
Evaluated value	$\bar{\sigma}^U = 0,0209 \pm 0,0008$ mb			Evaluated value	$\bar{\sigma}^U = 0,428 \pm 0,006$ mb			Recommended value	$\bar{\sigma}^U = 0,096 \pm 0,008$ mb		

Note: The symbols (S), (Fe), (Ni) and (Al) stand for the reactions $^{32}\text{S}(n, p)^{32}\text{P}$, $^{54}\text{Fe}(n, p)^{54}\text{Mn}$, $^{58}\text{Ni}(n, p)^{58}\text{Co}$ & $^{27}\text{Al}(n, \alpha)^{24}\text{Na}$.

Table 2. Decay characteristics of reaction products

Nuclide	Half-life	Photon energy, MeV	Emission, %
^{48}Sc	43,8 h	1,312	100
^{89}Zr	78,43 h	0,909	99
$^{92}\text{Nb}^{\#}$	10,13 d	0,934	99,2

Table 3. Mean cross-sections for reactions in the ^{252}Cf spectrum, mb

Reaction	Ref.	$\bar{\sigma}^{cf}$	$\bar{\sigma}^U$ (conversion from $\bar{\sigma}^{cf}$)
$^{51}\text{V}(n, \alpha)^{48}\text{Sc}$	[9]	0,043±0,02	0,0244
$^{93}\text{Nb}(n, 2n)^{92}\text{Nb}^{\#}$	[9]	0,88±0,04	0,483
$^{90}\text{Zr}(n, 2n)^{89}\text{Zr}$	[9]	0,267±0,015;	0,130
	[10]	0,221±0,006	0,108

Table 4. Calculated integral reaction cross-sections, mb

Reaction	$E_{\text{eff.}}$ MeV	σ_{eff}	$\bar{\sigma}^U$	$\bar{\sigma}^{cf}$
$^{51}\text{V}(n, \alpha)^{48}\text{Sc}$	9,0	8,0	0,0217	0,0375
$^{93}\text{Nb}(n, 2n)^{92}\text{Nb}^{\#}$	10,5	470,0	0,427	0,778
$^{90}\text{Zr}(n, 2n)^{89}\text{Zr}$	13,0	720,0	0,102	0,209

cross-sections for reactions in the ^{235}U [11] and ^{252}Cf [13] spectra and cross-sections from the library in Ref. [12]. There is satisfactory agreement between these and the evaluation of the experimental mean cross-sections obtained in this paper. The calculated values of the effective thresholds and reaction cross-sections are given, and the spread of effective cross-sections for a wide range of spectra from the BKS-2 library [11] is not more than 3% of the indicated effective thresholds.

REFERENCES

- [1] GRIGOR'EV, E.I., TARNOVSKIY, G.B., YARYNA, V.P., Measurements of the mean cross-sections of threshold reactions for ^{235}U fission neutrons [in Russian]. In: Neutron physics: Proceedings of the Sixth All-Union Conference on Neutron Physics, Kiev, 2-6 October 1983, Vol. 3, TsNIIatominform, Moscow (1984) 187-190.
- [2] ROY, J.C., HAWTON, J.J., Rep. CRC-1003, (1960).
- [3] NASYROV, F., At. Ehnerg., 25 (1968) 437.

- [4] KIMURA, I., et al., NST, 8 (1971) 59.
- [5] KOBAYASHI, K., et al., *ibid.*, 3 (1976) 531.
- [6] FABRY, A., et al., Neutron cross-section for reactor dosimetry. IAEA-208 Vol. 1 (1978) 233.
- [7] DE REGGE, P., et al., Radiochim. Acta, 17 (1972) 69.
- [8] QAIM, S.M., et al., Chem. nucl. data measurem. and appl., (1971) 121.
- [9] DERSO, Z., CSICAI, J., in: Neutron physics: Proceedings of the Fourth Conference on Neutron Physics, Kiev, 18-22 April 1977, Atomizdat, Moscow (1977) 32.
- [10] MANNHART, W., Radiation metrology techniques, data bases and standardization: Proc. Fourth ASTM-EURATOM Symp. on Reactor Dosimetry, Vol. 2 (1982) 637.
- [11] GRIGOR'EV, E.I., et al., in: Proceedings of the Third All-Union Meeting on Neutron Radiation Metrology in Reactors and Accelerators, Vol. 2, TsNIIatominform, Moscow (1983) 215.
- [12] BYCHKOV, V.M., et al., Manual of neutron-induced threshold reaction cross-sections [in Russian], Ehnergoizdat, Moscow (1982).
- [13] Nuclear Data Standards for Nuclear Measurements. Technical Reports Series No. 227, IAEA, Vienna (1983).

APPROXIMATION OF THE CROSS-SECTIONS FOR CHARGED-PARTICLE EMISSION
REACTIONS NEAR THE THRESHOLD

S.A. Badikov, A.B. Pashchenko

The paper analyses the recommended cross-sections for threshold reactions [1] with charged-particle emission, which are among those used most in neutron metrology and reactor dosimetry problems. Various circumstances made it necessary to review the excitation functions of some reactions represented in the BOSPOR library. It should be noted that the recommended or evaluated nuclear data objectively reflect the level of experimental information and model representations regarding nuclear reaction mechanisms that existed at the time they were obtained. In recent years there have appeared new differential and integral experimental data which fully confirm the reliability of the evaluation made [1] and, in some cases, refine the recommended cross-sections in the BOSPOR library.

We note that the recommended excitation functions for threshold reactions with charged-particle emission in the BOSPOR library have one common fault - they start from some threshold value of the incident neutron energy (effective reaction threshold) which is always somewhat higher than the corresponding energy threshold, whereas a correct understanding of the nuclear reaction mechanism assumes that the excitation function of a threshold reaction should have very small but non-zero values in the range from the energy threshold to the effective threshold of reaction. The cross-section evaluation method involving theoretical models, used by the authors in setting up the BOSPOR library, did not permit a correct determination of cross-sections below the effective reaction threshold. In most practical cases, this is of no consequence since, according to our evaluations, the contribution, for example, of the value of the tail (neglected earlier) to the cross-section averaged over the reactor neutron spectrum is of the order of 0.1%. However, for some problems of neutron metrology (for example, in unfolding neutron spectra on the basis of measured reaction velocities) it is more

correct to take into account the cross-sections in the near-threshold energy region right up to the energy threshold of the reaction. This will give us a physically correct representation of the energy dependence of the recommended cross-sections for charged-particle emission reactions over the entire interval of incident neutron energies.

Therefore, in the present work, we performed an analytical approximation of their energy dependence to the reaction threshold for the (n,p) and (n,α) reaction cross-sections of the BOSPOR library, corrected with allowance for the latest differential and integral experiment data, using the common features characteristic of the energy dependence of the threshold reaction cross-sections, and making some physical assumptions.

Method of approximation of cross-sections to the reaction threshold

The approximation method used by the authors permits calculation of the cross-sections for the (n,p) and (n,α) reactions with charged-particle emission deep below the barrier. We will consider the calculation scheme for endothermic reactions. Similar considerations are valid for exothermic reactions; the formulae corresponding to the latter will be marked by a prime.

For our approximation we chose the segment $[Q, Q + B]$ (for exothermic reactions $[OB]$), where Q is the reaction threshold and B the Coulomb barrier height. In determining the form of the approximant and the segment of approximation, the following factors were taken into consideration:

- Availability of reliable evaluated data on the energy dependence of the cross-section in the greater part (usually 2/3) of the segment $[Q, Q + B]$;
- Monotonic increase in the excitation function of the nuclear reaction under the influence of the Coulomb barrier, in the segment $[Q, Q_1]$ where the cross-section is to be calculated;
- Asymptotic behaviour of the cross-section near the threshold (endothermic reactions) and at neutron energies not too close to zero (exothermic reactions).

It is known from Refs [2, 3] that the endothermic reaction cross-section in the region referred to varies according to the law

$$\sigma(E) \sim \sqrt{E-Q} \exp\left(-\sqrt{2} \pi Z_B Z_b \ell^2 \sqrt{\mu} / \hbar \sqrt{E-Q}\right), \quad (1)$$

and the exothermic reaction cross-section according to the law

$$\sigma(E) \sim \exp\left(-\sqrt{2} \pi Z_B Z_b \ell^2 \sqrt{\mu} / \hbar \sqrt{E+Q}\right), \quad (1')$$

where E is the energy of relative particle motion, $Z_B \ell$, $Z_b \ell$ are the charges of the residual nucleus and charged particle, $\mu = m_B m_b / (m_B + m_b)$ is their reduced mass \hbar is the Planck constant.

The cross-sections in the sub-barrier region are calculated in several steps:

1. The cross-section in the interval under study is represented in the form

$$\sigma(E) = \sqrt{E-Q} T_0(E-Q) g(E); \quad (2)$$

$$\sigma(E) = T_0(E+Q) g(E), \quad (2')$$

which takes into account the influence of the main physical factors - the presence of the reaction threshold and Coulomb barrier. The function $g(E)$ describes the action of neglected factors. In formulae (2) and (2') $T_0(E)$ is the penetrability of the Coulomb barrier for protons and alpha particles with orbital moment $\ell = 0$ calculated for a potential of the form

$$V(z) = \begin{cases} \frac{Z_B Z_b \ell^2}{z}, & z \geq R; \\ -V_0 & z < R \end{cases} \quad (3)$$

by the method of Ref. [4]:

$$T_0(E) = \exp[-\alpha(E)] / \{1 + \exp[-\alpha(E)]\}. \quad (4)$$

here

$$\alpha(E) = (2\sqrt{2}\mu R Z_B Z_b \ell^2 / \hbar) (\sqrt{\beta} \arctg \sqrt{\beta-1} - \sqrt{1-1/\beta}), \quad (5)$$

where $\beta = Z_B Z_b \ell^2 / RE$; $R = r_0 A^{1/3}$ ($r_0 = 1.4 \times 10^{-15}$ μ , and A is the relative atomic mass of the residual nucleus). In this case, a smoother dependence $g(E)$ was obtained than when the formula for penetrability in the ordinary quasi-classical approximation was used.

Formulae (1) and (1') were obtained on the assumption that the nuclear potential satisfied a single condition: that it should be concentrated in a limited region [3]. Therefore, the simplest form of nuclear interaction was used in the calculations - a potential well of finite depth. Note also that representations (2) and (2') are valid in a wider energy region than similar relations including the exponential multiplier

$$\sigma(E) = \sqrt{E-Q} \exp(-\sqrt{2} \pi Z_B Z_b \ell^2 \sqrt{\mu} / \hbar \sqrt{E-Q}) g(E); \quad (6)$$

$$\sigma(E) = \exp(-\sqrt{2} \pi Z_B Z_b \ell^2 \sqrt{\mu} / \hbar \sqrt{E+Q}) g(E). \quad (6')$$

For small values of $E-Q$ and $E+Q$ expressions (2) and (2') with penetrabilities calculated by formulae (4) and (5) turn, respectively, into expressions (6) and (6').

2. The function $g(E)$ is selected in the $[Q, Q+B]$ interval on the basis of the recommended energy dependence of the cross-section [1]. In Fig. 1 the broken line indicates the possible variants of the behaviour of $g(E)$. The procedure of selection of dependence $g(E)$ served only one purpose - to obtain a function whose logarithm had a substantially weaker dependence on energy than $\lg \sigma(E)$.

There is no doubt that the penetrabilities calculated in the approximation under consideration differ from those corresponding to the hypothetical "true" potential. This follows from Fig. 1,c, which gives the behaviour of function $g(E)$ most characteristic of this series of calculations. In fact, the dependence $g(E)$ increases rapidly near the value Q_1 in the interval where the quasi-classical approximation [$T_0(E) \ll 1$] is valid. At the same time, in this region its dependence on energy should be

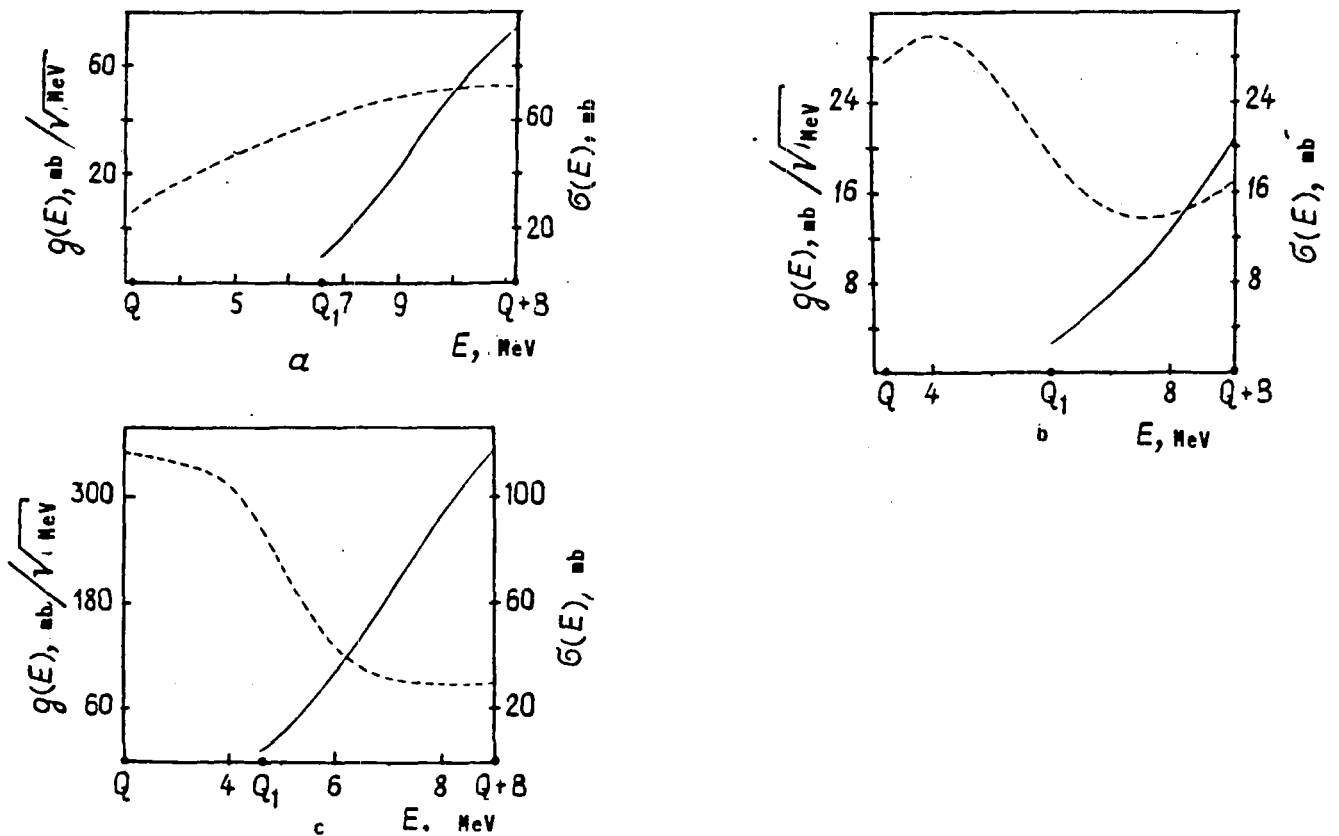


Fig. 1. Results of extrapolation of the function $g(E)$ (broken line) to the $[Q, Q_1]$ region for reactions: (a) $^{27}\text{Al}(n, \alpha)^{24}\text{Na}$; (b) $^{48}\text{Ti}(n, p)^{48}\text{Sc}$; (c) $^{60}\text{Ni}(n, p)^{60}\text{Co}$. Continuous curves - evaluated reaction cross-sections from BOSPOR library.

weak since the cross-section is determined here mainly by the Coulomb barrier penetrability for charged particles with orbital moment $l = 0$. Nevertheless, dependences (2) and (2'), taking into account expressions (4) and (5), can be used to describe with sufficient accuracy (to within 1.5%) the evaluated values of cross-sections in the $[Q_1, Q + B]$ interval and to calculate the unknown cross-section values in the $[Q, Q_1]$ interval which satisfy the integral experiments.

3. The dependence $g(E)$ is approximated in the $[Q_1, Q + B]$ interval by the rational function $g_a(E)$ with the use of the PADE 2 program [5]. The approximant $g_a(E)$ is extrapolated to region $[Q, Q_1]$.

4. The cross-section in the $[Q, Q_1]$ region is calculated by the formulae $\sigma_a(E) = \sqrt{E - Q} T_0(E - Q) g_a(E)$ and $\sigma_a(E) = T_0(E + Q) g_a(E)$.

Thus, the problem of calculation of cross-sections in the sub-barrier region is, in fact, a problem of extrapolation of the function $g(E)$ in the

$[Q, Q_1]$ interval since the required behaviour of cross-sections near the threshold is ensured by the multiplier $T_0(E)$. The extrapolation of an approximately known function belongs to the class of incorrectly posed problems [6]. Therefore, a sufficiently accurate (to within 1.5%) determination of the dependence $g(E)$ in the $[Q_1, Q + B]$ interval is no guarantee for an equally accurate reproduction of the function $g(E)$ in the $[Q, Q_1]$ interval. There is a set of functions $\{g_a^i(E)\}$ with appropriate behaviour in the $[Q_1, Q + B]$ region. In order to choose a solution from this set, we need additional data, and we used for this purpose the evaluated integral data together with the requirement that the extrapolation of $g_a(E)$ should be positive and monotonic.

Comparison of the results with the integral data and discussion

Evaluated microscopic nuclear data are generally tested against the results of integral experiments, because these are usually more accurate. In order to analyse the wide range of the dependence of microscopic cross-sections on the energy of interacting neutrons, we must use integral measurements in neutron spectra of various forms differing in the "degree of hardness".

An international co-ordinated programme of microscopic cross-section evaluation for reactor dosimetry and integral experiments in standard neutron fields (the Benchmark Programme) has been prepared [7] and is being implemented [8]. The decisive condition for using integral experiment results to verify differential cross-sections is that the characteristics of the neutron field in which the measurement is carried out should be sufficiently complete. The thermal fission neutron spectrum of ^{235}U is the one which has been studied most.

Approximation of the thermal fission neutron spectrum of ^{235}U and averaging of cross-sections

The spectrum-averaged cross-section is determined by the formula $\bar{\sigma} = \int_0^{\infty} \sigma(E)\chi(E)dE$, where σE is the reaction cross-section, and $\chi(E)$ is the normalized [$\int_0^{\infty} \chi(E)dE = 1$] neutron spectrum.

The neutron spectrum in the present work was approximated by the following formulae:

$$\chi_1(E) = 0,48395 \exp(-E) \sinh \sqrt{2E} \quad - \text{Watt's formula [9];}$$

$$\chi_2(E) = 0,45274 \exp(-E/0,965) \sinh \sqrt{2,29E} \quad - \text{Cranberg's formula [10];}$$

$$\chi_3(E) = 0,76985 \exp(-0,775E) \sqrt{E} \quad - \text{Lichman's formula [11];}$$

The uncertainty in the description of the neutron spectrum reflects the status of the experimental data. The greatest error is observed in the very soft and hard parts of the spectrum.

The evaluations used more frequently of late for approximation of the ^{235}U fission neutron spectrum are those of the NBS [13] and the ENDF/B-V library [13], which are recommended by the IAEA [12] and included in the international reactor dosimetry file (IRDF).

Evaluated integral cross-sections

In selecting the recommended values of integral cross-sections in the ^{235}U fission neutron spectrum, the authors were guided mainly by the results of Refs [14-16]. In addition, they used the integral cross-section evaluation results published in Refs [17, 18].

In Ref. [14] the integral microscopic cross-sections measured on the ^{235}U thermal fission neutron spectrum for the 29 threshold reactions which are most important in reactor dosimetry and fast reactor technology were evaluated. Most of the integral measurements were carried out by the relative method and therefore their results were renormalized in Ref. [14].

Table 1

Comparison of the recommended excitation functions of threshold reactions with charged-particle emission averaged over the ^{235}U fission neutron spectrum with experimental data

Reaction	Averaged cross-section, mb						
	Evaluated Experiment	BOSPOR-80 library			Results after correction and approximation of cross-sections		
		$\chi_1(E)$	$\chi_2(E)$	$\chi_3(E)$	$\chi_1(E)$	$\chi_2(E)$	$\chi_3(E)$
$^{24}\text{Mg}(np)^{24}\text{Na}$	1,50 \pm 0,06 [16]	1,52	1,40	1,56	1,60	1,48	1,63
$^{27}\text{Al}(n\alpha)^{24}\text{Na}$	0,706 \pm 0,028 [16]	0,698	0,638	0,724	0,738	0,676	0,762
$^{27}\text{Al}(np)^{27}\text{Mg}$	3,95 \pm 0,20 [16]	3,99	3,82	3,83	4,06	3,89	3,90
$^{31}\text{P}(np)^{31}\text{Si}$	35,5 \pm 2,7 [15]	32,5	32,0	30,6	32,36 ⁺	32,86	30,55 ⁺
$^{32}\text{S}(np)^{32}\text{P}$	66,8 \pm 3,7 [15]	65,62	64,47	61,94	65,49 ⁺	64,33 ⁺	61,81 ⁺
$^{46}\text{Ti}(np)^{46}\text{Sc}$	11,6 \pm 0,4 [16]	12,81 (11,15)	12,28 (10,67)	12,25 (10,69)	- 11,23	- 10,74	- 10,77
$^{47}\text{Ti}(np)^{47}\text{Sc}$	17,7 \pm 0,6 [16]	22,2	21,8	21,0	22,21	21,86	21,09
$^{48}\text{Ti}(np)^{48}\text{Sc}$	0,302 \pm 0,010 [16]	0,262 (0,282)	0,241 (0,260)	0,269 (0,289)	- 0,285	- 0,263	- 0,292
$^{54}\text{Fe}(np)^{54}\text{Mn}$	80,5 \pm 2,3 [16]	82,2	80,4	77,7	82,52	80,76	78,02
$^{56}\text{Fe}(np)^{56}\text{Mn}$	1,09 \pm 0,04 [16]	1,078	1,004	1,078	1,070 ⁺	0,999 ⁺	1,070 ⁺
$^{59}\text{Co}(n\alpha)^{56}\text{Mn}$	0,161 \pm 0,007 [16]	0,147	0,135	0,151	0,157	0,145	0,161
$^{58}\text{Ni}(np)^{58}\text{Co}$	105,1 \pm 1,1 [18]	103,0	101,0	97,9	103,6	101,5	98,0
$^{60}\text{Ni}(np)^{60}\text{Co}$	2,3 \pm 0,4 [17]	2,57	2,42	2,53	2,59	2,43	2,54
$^{63}\text{Cu}(n\alpha)^{60}\text{Co}$	0,500 \pm 0,056 [15]	0,482	0,452	0,478	0,493	0,462	0,488
$^{64}\text{Zn}(np)^{64}\text{Cu}$	30,2 \pm 0,5 [18]	36,8 (32,02)	36,0 (31,25)	34,8 (30,25)	- 32,24	- 31,46	- 30,48
$^{90}\text{Zr}(np)^{90}\text{Y}$	0,38 \pm 0,02 [19]	0,33 (0,36)	0,31 (0,33)	0,33 (0,35)	- 0,37	- 0,34	- 0,36

Remarks:

(1) The results after correction of the cross-sections on the basis of integral data are given in brackets. (2) The plus sign indicates the cross-section values which are smaller than the corresponding averaged cross-sections of BOSPOR-80. The deviations are within the accuracy of approximation.

The recommended values of the spectrum-averaged cross-sections were obtained in Ref. [14] by root-mean-square averaging of the available experimental data, taken with a "weight" equal to the indicated experimental error and renormalized by the authors.

The data recommended in Ref. [17] include the results of the evaluation in Ref. [14] without any changes except for the cross-section error, which in Ref. [17] takes into account the uncertainty of the standard. Moreover, Ref. [17] analysed all accessible integral cross-section measurements on the ^{235}U fission neutron spectrum published up to 1974, and evaluated these cross-sections by a method similar to that applied in

Ref. [14]. The same values of standards were used in renormalizing the cross-sections.

In Ref. [16] the results of new measurements of the ^{235}U spectrum-averaged cross-sections were published for 17 threshold reactions. After appropriate correction for multiple scattering, sample thickness and other secondary effects, it was found that for most elements the measurement results agreed satisfactorily with the results of the integral cross-section evaluation performed earlier by the same authors.

There is, on the whole, satisfactory agreement between the recommended cross-sections averaged over the ^{235}U thermal fission spectrum and the results of the integral experiments (see Table 1). The approximation of the cross-sections for charged-particle emission reactions to the reaction threshold in most cases makes a contribution of less than 1% to the integral cross-section.

REFERENCES

- [1] BYCHKOV, V.M., ZOLOTAREV, K.I., PASHCHENKO, A.B., et al., Organization of the computerized library of evaluated threshold reaction cross-sections BOSPOR-80 and its testing using integral experiments, Vopr. At. Nauki i Tekhniki: Ser. Yad. Konstanty 3(42) (1981) 60. [in Russian]
- [2] DAVYDOV, A.S., The Theory of the Atomic Nucleus, Fizmatgiz, Moscow (1958) 254. [in Russian]
- [3] BAZ', A.I., ZEL'DOVICH, Ya.B., PERELOMOV, A.M., Scattering, Reactions and Decays in Non-relativistic Quantum Mechanics, Nauka, Moscow (1971) 389. [in Russian]
- [4] PONOMAREV, L.I., Lectures on Quasi-classical Physics, Rep. ITF-53 (1967) 24. [in Russian]
- [5] BADIKOV, S.A., et al., The Rational Approximation Program PADE2, Rep. FEhI-1686, Obninsk (1985). [in Russian]
- [6] TIKHONOV, A.N., ARSEININ, V.Ya., Methods for Solving Certain Problems, Nauka, Moscow (1979). [in Russian]
7. Rep. INDC (SEC)-54/LADOS, July 1976.
8. Neutron cross-sections for reactor dosimetry. V.I, II: Rep. IAEA-208. Vienna, 1978.
9. Reynolds S.A., Emery J.P., Wyatt E.L. Half-lives of radionuclides. - Nucl.Sci. and Engng, 1968, v.32, p.46.

10. Ryves T.B. Activation measurements of thermal neutron capture cross-sections and resonance integrals. - J.Nucl.Energy, 1970, v.24, p.35.
 11. Story J.S. Winfrith nuclear data group notes on topics in nuclear data evaluation, 1964-1968: Rep. AEEW-M-7907, 1968.
 12. Cullen D.E., Kocherov N., McLaughlin P.K. The international reactor dosimetry file (IRDIF-82): Rep. IAEA-IDS-41, 1982.
 13. IAEA group meeting on nuclear data for reactor dosimetry (Vienna, 13-17 November 1978). Vienna, 1979: Rep. INDC(NDS)-100/m.
 14. Fabry A. Rep. RLG-465, 1972.
 15. Parby A., McElroy W.N., Kellogg L.S. e.a. Rev. of microscopic integral cross-sections data in fundamental reactor dosimetry benchmark neutron fields. - In: Proc. of a consultants meeting on integral cross-section measurement in standard neutron fields for reactor dosimetry (Vienna, 15-19 November 1976). V.1, Vienna, 1978, p.233: Rep. IAEA-208.
 16. Mannhart W., Parby A. U-235 spectrum-averaged neutron cross-sections, 1985, v.V, p.58: Rep. NEANDC(E)-262 U.
 17. Calamand A. Cross-sections for fission neutron spectrum induced reactors. Vienna: IAEA, 1973: Rep. INDC(NDS)-55L.
- [18] BONDARS, Kh.Ya., LAPENAS, A.A., Recommended Cross-sections for Activation Detectors. Rep. LAFI 054, 057, Salaspils (1983). [in Russian]
- [19] BONDARS, Kh.Ya., WEINBERG, Ya.K., LAPENAS, A.A., Activation cross-sections for some threshold reactions, Vopr. At. Nauki i Tekhniki: Ser. Yad. Konstanty 15 (1974) 63. [in Russian]

GROUP CONSTANTS FOR ^{233}U , ^{235}U and ^{239}Pu IN THE RESONANCE REGION

A.A. Van'Kov, V.V. Kolesov, V.F. Ukraintsev

At present we are seeing a slowing down in the arrival of new experimental information on nuclear data for reactor materials. This is said to be due to the difficulty of setting up essentially new experiments, and also to the partial meeting of reactor nuclear data requirements. In this situation there is an urgent need to develop calculation methods and programs for the preparation of group constants based on neutron cross-section parameter information. The present paper gives the results of group constant calculations for three fissile nuclides prepared using the method of joint analysis of neutron cross-sections and transmission functions in a multilevel model. Reference [1] describes the methods for analysing the neutron cross-sections of heavy nuclides in the unresolved resonance region, and Ref. [2] does the same for the resolved region [2]. The latter analysis led to an evaluation of resonance parameters for ^{239}Pu [3].

The analytical approach was generally as follows - the parameters of the theoretical model were evaluated on the basis of experimental information on mean neutron cross-sections and transmission functions; then, group constants were calculated using an accurate theoretical model. The parameter sensitivity coefficients for all functionals (transmission and self-indication functions, group constants) were calculated simultaneously. The new features of the approach were as follows:

- Careful statistical evaluation (mean values and covariance matrices) of mean resonance parameters and group constants;
- Use of a suitably accurate theoretical model which allows for inter-level interference effects;
- Incorporation in the analysis of experimental information on transmission and self-indication functions, which makes for significantly greater accuracy in the resonance self-shielding factors.

In this way, self-consistent evaluations of the values and errors of the resonance parameters and group constants were obtained. In the nuclear data evaluation literature for fissile nuclides in the unresolved resonance region, the authors stay within the framework of a simplified theoretical model of the Hauser-Feshbach type which does not allow resonance self-shielding factors to be evaluated and does not take inter-level interference into account. Therefore, in existing group constant tables (see, for example, Ref. [4]) the evaluations of mean cross-sections, on the one hand, and of resonance self-shielding factors and their temperature dependence, on the other, are not self-consistent.

The present paper gives evaluations of group constants in the unresolved resonance region for ^{233}U , ^{235}U , and ^{239}Pu drawing on up-to-date recommended data on mean cross-sections and transmission functions (the latter were measured for ^{235}U and ^{239}Pu). For ^{239}Pu , these group constant evaluations extend right up to the thermal neutron energy region. This was made possible thanks to the use of an improved S-matrix formalism when evaluating the resonance parameters. Experimental data for other fissile nuclides in the resolved region are not good enough to permit an analogous approach to be employed with the same degree of reliability.

Available data on mean resonance parameters, and in particular, for ^{233}U , the evaluations given in Ref. [5], were used as a priori information in the unresolved resonance region. Note that there is no information in Ref. [4] on this nuclide which is so important for research into the thorium cycle. For ^{235}U , we worked from the mean cross-section data on which the evaluations in ENDF/B-V [6] are based, and for ^{239}Pu , from the data given in Ref. [4], since they are the most up to date.

Mean resonance parameters. The data in Ref. [5] were used for ^{233}U , and no fitting was done owing to the lack of experimental information on mean cross-sections. These parameters do not depend on energy: the mean radiation width $\bar{\Gamma}_\gamma$, which is the same in all states and equals 0.039 eV; the

potential scattering radius $R' = 9.93$ fm; and the mean distance between S-resonances $\bar{D} = 6.80$ eV. The law of proportionality was assumed for the different states $J : D_J \approx 1(2J + 1)$. The remaining parameters (the strength functions S_0, S_1 and the fission widths) are given in the form of fluctuating values in a fine-group partition for the 0.1-30 keV range.

The mean resonance parameters for ^{235}U were optimized in the light of the experimental data on the transmission and self-indication functions for the fission reaction given in Ref. [7]. The following evaluations were obtained for the parameters which do not depend on energy: the mean radiation width $\bar{\Gamma}_\gamma = 30 \pm 2$ MeV (for all states), the p-strength function $S_1 = 1.68 \pm 0.45 \times 10^{-4}$, and the mean distance between S-resonances $\bar{D} = 440 \pm 20$ MeV. Including the transmission functions in the calculations meant that the monotonic energy dependence of the potential scattering radius R' on the neutron energy had also to be introduced. In addition, it was found that the observed mean cross-sections could only be described using fluctuating values (from group to group) for the S-strength function and fission widths. The average value for the S-strength function over a wide lethargy interval was found to be $S_0 = 0.97 \pm 0.05 \times 10^{-4}$, and the scattering radius $\bar{R}' = 9.3 \pm 0.1$ fm.

An analogous optimization process was performed for ^{239}Pu . The experimental data used here are given in Ref. [8], where preliminary evaluations are also given of the parameters and of certain constants for ^{239}Pu (done by "manual" fitting). The present paper gives definitive statistical evaluations of: $\Gamma_\gamma = 39.5 \pm 4.0$ MeV, $S_1 = 2.17 \pm 0.40 \times 10^{-4}$ (these parameters are not dependent on neutron energy), $\bar{R}' = 9.2 \pm 0.2$ fm (this parameter is monotonically dependent on neutron energy), $\bar{S}_0 = 0.98 \pm 0.06 \times 10^{-4}$ (fluctuating parameter). The fission widths varied from group to group.

The fluctuation in the strength functions indicate that the processes which occur when neutrons interact with fissile nuclei are highly complex. Experience shows, that for even-even (non-fissile) nuclei, a good description

Table 1

Mean-group cross-sections for the nuclides ^{239}Pu , ^{235}U , ^{233}U in the unresolved resonance region, burns

Group No.	E, keV	^{239}Pu				^{235}U				^{233}U			
		σ_t	σ_f	σ_c	σ_{el}	σ_t	σ_f	σ_c	σ_{el}	σ_t	σ_f	σ_c	σ_{el}
11	10-21,5	14,77	1,82	0,932	12,02	14,70	2,60	1,10	11,0	16,40	3,14	0,562	12,7
12	4,65-10	16,51	2,14	1,573	12,8	16,39	3,42	1,37	11,6	18,04	4,20	0,739	13,1
13	2,15-4,65	19,15	2,92	2,53	13,7	18,82	5,12	1,70	12,0	22,37	7,02	1,35	14,0
14	1-2,15	22,9	4,35	4,07	14,5	22,44	7,13	2,91	12,4	27,36	10,8	2,16	14,4
15	0,465-1	29,97	8,14	6,23	15,6	28,48	11,4	4,58	12,5	30,64	13,4	2,94	14,3
16	0,215-0,465	-	-	-	-	36,30	16,2	7,40	12,7	35,04	17,6	3,34	14,1
17	0,100-0,215	-	-	-	-	46,6	21,6	11,5	13,5	58,49	34,8	8,79	14,9

of the mean cross-sections can be obtained with constant strength function values.

Group constants for ^{233}U , ^{235}U and ^{239}Pu in the unresolved

resonance region. Table 1 gives the mean-group cross-sections for the nuclides under investigation (in the ABBN groups [4]). They differ but little from the primary data on which the mean neutron cross-section evaluations are based. Our results differ from the data given in Ref. [6] for ^{235}U by no more than 5%, and from those given in Ref. [4] for ^{239}Pu by no more than 10%.

The following tables give information which is based on a new methodology (resonance self-shielding factors as a function of dilution cross-section and temperature). These data differ from those in Ref. [4] in that they have been obtained using a unified procedure for evaluating the primary information (mean cross-sections and transmission functions) and a suitably accurate theoretical model.

Table 2 gives data on resonance self-shielding factors for three nuclides for different dilution cross-sections at room temperature. When these data are compared with the results given in Ref. [4] it is seen that, for ^{235}U , they are systematically lower, and that for ^{239}Pu the opposite obtains. The temperature (Doppler) increments for these factors are given in Table 3. They are significantly lower than the corresponding data in Ref. [4]. The difference is particularly large (factor of 1.5-2) for a zero

Table 2

Resonance self-shielding factors as a function of dilution cross-section at a temperature of 300 K (in burns)

Group No.	$f_t(\sigma_0)$				$f_f(\sigma_0)$				$f_c(\sigma_0)$				$f_{el}(\sigma_0)$			
	0	10	10 ²	10 ³	0	10	10 ²	10 ³	0	10	10 ²	10 ³	0	10	10 ²	10 ³
<u>233_U</u>																
11	0,897	0,935	0,984	0,994	0,931	0,957	0,990	0,999	0,926	0,953	0,989	0,999	0,951	0,970	0,993	0,999
12	0,888	0,927	0,981	0,993	0,910	0,941	0,985	0,998	0,898	0,932	0,982	0,998	0,954	0,971	0,993	0,999
13	0,818	0,870	0,960	0,992	0,831	0,880	0,965	0,996	0,803	0,858	0,957	0,995	0,944	0,962	0,989	0,999
14	0,776	0,826	0,934	0,967	0,784	0,836	0,944	0,992	0,736	0,796	0,926	0,990	0,952	0,964	0,987	0,998
15	0,712	0,766	0,900	0,963	0,714	0,775	0,914	0,987	0,661	0,726	0,887	0,982	0,956	0,966	0,986	0,998
16	0,667	0,723	0,871	0,960	0,688	0,749	0,896	0,984	0,591	0,657	0,841	0,972	0,963	0,971	0,987	0,998
17	0,461	0,516	0,702	0,911	0,544	0,604	0,787	0,953	0,441	0,498	0,696	0,924	0,903	0,915	0,948	0,985
<u>235_U</u>																
11	0,889	0,933	0,984	0,999	0,927	0,957	0,990	0,999	0,924	0,955	0,990	0,999	0,948	0,969	0,993	0,999
12	0,877	0,924	0,981	0,998	0,909	0,943	0,987	0,999	0,905	0,941	0,986	0,999	0,948	0,968	0,993	0,999
13	0,855	0,905	0,974	0,997	0,874	0,917	0,978	0,998	0,864	0,909	0,975	0,997	0,954	0,971	0,993	0,999
14	0,809	0,861	0,955	0,991	0,819	0,871	0,961	0,995	0,799	0,855	0,955	0,995	0,956	0,969	0,991	0,999
15	0,697	0,764	0,909	0,962	0,729	0,795	0,928	0,990	0,703	0,772	0,917	0,988	0,944	0,958	0,985	0,998
16	0,573	0,645	0,832	0,952	0,622	0,697	0,873	0,980	0,599	0,673	0,858	0,976	0,927	0,941	0,973	0,995
17	0,478	0,543	0,747	0,931	0,548	0,622	0,822	0,967	0,484	0,557	0,770	0,952	0,922	0,933	0,964	0,992
<u>239_{Pu}</u>																
11	0,843	0,902	0,975	0,998	0,895	0,936	0,985	0,998	0,861	0,914	0,979	0,998	0,922	0,952	0,989	0,999
12	0,779	0,852	0,956	0,998	0,822	0,855	0,970	0,997	0,776	0,852	0,960	0,995	0,894	0,930	0,981	0,998
13	0,713	0,788	0,922	0,993	0,734	0,813	0,943	0,993	0,654	0,749	0,918	0,989	0,871	0,907	0,968	0,996
14	0,634	0,698	0,859	0,986	0,618	0,706	0,889	0,984	0,516	0,617	0,847	0,977	0,849	0,880	0,949	0,992
15	0,498	0,555	0,732	0,906	0,482	0,569	0,794	0,961	0,354	0,445	0,714	0,943	0,789	0,818	0,898	0,977

dilution cross-section. Hence, we may conclude that the positive component of the Doppler coefficient of reactivity for fissile nuclei is in reality significantly smaller than it appears when calculated from the constants given in Ref. [4], which is a matter of some importance for reactor construction.

Group constants for ²³⁹Pu in the resolved resonance region.

Reference [2] describes a method for the joint evaluation method of neutron cross-sections for the nuclide ²³⁹Pu in the resolved resonance region using an improved S-matrix theory. This evaluation procedure is special in that the results are tested against measurements of the averaged fission reaction transmission and self-indication functions (as with the results above for the unresolved resonance region). This makes for greater reliability when calculating resonance self-shielding factors and their temperature dependence.

Table 3

Doppler increments of resonance self-shielding factors for ²³³U as a function of dilution cross-section

Group No.	$\Delta f_t(\sigma_0)$				$\Delta f_f(\sigma_0)$				$\Delta f_c(\sigma_0)$				$\Delta f_{el}(\sigma_0)$			
	0	10	10 ²	10 ³	0	10	10 ²	10 ³	0	10	10 ²	10 ³	0	10	10 ²	10 ³
²³³ U																
II	0,007	0,004	0,001	0,001	0,010	0,007	0,001	0	0,012	0,008	0,002	0	0,002	0,001	0	0
	0,004	0,002	0,001	0	0,006	0,004	0,001	0	0,006	0,004	0,001	0	0,001	0	0	0
12	0,014	0,010	0,003	0,001	0,021	0,014	0,004	0,001	0,025	0,017	0,005	0,001	0,003	0,002	0,001	0
	0,008	0,005	0,001	0	0,011	0,007	0,002	0,002	0,013	0,008	0,002	0	0,001	0,001	0	0
13	0,026	0,021	0,008	0,002	0,035	0,026	0,009	0,001	0,046	0,035	0,012	0,002	0,005	0,004	0,002	0
	0,017	0,013	0,005	0,001	0,022	0,016	0,005	0,001	0,026	0,019	0,006	0,001	0,003	0,002	0,001	0
14	0,041	0,035	0,017	0,003	0,050	0,039	0,015	0,002	0,055	0,024	0,004	0,001	0,008	0,006	0,003	0,001
	0,033	0,027	0,011	0,002	0,036	0,028	0,010	0,001	0,037	0,014	0,002	0,001	0,006	0,005	0,002	0
15	0,045	0,041	0,024	0,005	0,056	0,047	0,022	0,004	0,075	0,065	0,033	0,060	0,007	0,006	0,003	0
	0,039	0,034	0,017	0,003	0,045	0,036	0,015	0,002	0,056	0,047	0,021	0,034	0,005	0,004	0,002	0
16	0,033	0,033	0,025	0,006	0,045	0,040	0,022	0,004	0,068	0,064	0,041	0,009	0,004	0,003	0,002	0,001
	0,033	0,031	0,019	0,004	0,041	0,035	0,017	0,003	0,056	0,050	0,027	0,005	0,003	0,003	0,002	0
17	0,035	0,038	0,040	0,019	0,051	0,048	0,035	0,011	0,067	0,068	0,012	0,022	0,006	0,006	0,006	0,003
	0,041	0,042	0,036	0,013	0,051	0,047	0,030	0,008	0,064	0,061	0,044	0,013	0,006	0,006	0,005	0,002
²³⁵ U																
II	0,007	0,004	0,001	0,001	0,009	0,005	0,001	0	0,009	0,006	0,001	0	0,002	0,001	0	0
	0,003	0,002	0,001	0	0,004	0,003	0,001	0	0,005	0,003	0,001	0	0,001	0	0	0
12	0,012	0,008	0,002	0,002	0,016	0,010	0,003	0	0,017	0,011	0,003	0	0,003	0,002	0	0
	0,007	0,004	0,001	0,001	0,009	0,006	0,001	0	0,010	0,006	0,002	0	0,001	0,001	0	0
13	0,022	0,016	0,005	0,002	0,030	0,021	0,006	0,001	0,031	0,022	0,007	0,001	0,004	0,003	0,001	0
	0,014	0,010	0,003	0,002	0,018	0,012	0,003	0	0,019	0,013	0,004	0	0,003	0,002	0,001	0
14	0,039	0,031	0,012	0,003	0,048	0,036	0,012	0,002	0,053	0,045	0,042	0,002	0,006	0,004	0,002	0
	0,026	0,020	0,007	0,002	0,030	0,022	0,007	0,001	0,033	0,020	0,019	0,001	0,004	0,003	0,001	0
15	0,060	0,052	0,026	0,006	0,070	0,056	0,023	0,034	0,078	0,064	0,027	0,004	0,009	0,008	0,004	0,001
	0,043	0,035	0,015	0,003	0,044	0,034	0,012	0,017	0,047	0,036	0,014	0,002	0,006	0,005	0,002	0
16	0,072	0,068	0,044	0,011	0,087	0,073	0,036	0,007	0,097	0,084	0,044	0,008	0,010	0,009	0,006	0,002
	0,061	0,053	0,029	0,006	0,063	0,052	0,023	0,004	0,066	0,055	0,025	0,004	0,008	0,007	0,004	0,001
17	0,062	0,066	0,058	0,019	0,088	0,080	0,048	0,011	0,097	0,091	0,061	0,016	0,010	0,009	0,007	0,003
	0,069	0,065	0,043	0,011	0,076	0,064	0,032	0,006	0,083	0,073	0,042	0,009	0,009	0,008	0,006	0,002
²³⁹ Pu																
II	0,020	0,014	0,004	0,002	0,020	0,013	0,003	0,001	0,030	0,020	0,006	0	0,010	0,007	0,002	0
	0,011	0,008	0,002	0,001	0,012	0,007	0,002	0	0,015	0,010	0,002	0,001	0,005	0,004	0,001	0
12	0,033	0,025	0,010	0,004	0,034	0,023	0,007	0	0,054	0,039	0,012	0,002	0,017	0,013	0,005	0
	0,020	0,015	0,005	0,002	0,021	0,014	0,004	0,001	0,029	0,020	0,006	0,001	0,010	0,007	0,002	0,001
13	0,045	0,041	0,023	0,007	0,055	0,043	0,016	0,002	0,090	0,074	0,030	0,004	0,024	0,021	0,010	0,001
	0,031	0,027	0,012	0,004	0,038	0,029	0,010	0,001	0,061	0,038	0,013	0,002	0,015	0,012	0,005	0,001
14	0,048	0,050	0,037	0,011	0,069	0,060	0,031	0,005	0,107	0,096	0,050	0,008	0,025	0,022	0,013	0,002
	0,042	0,039	0,023	0,007	0,054	0,044	0,018	0,003	0,074	0,062	0,027	0,005	0,010	0,017	0,009	0,002
15	0,037	0,044	0,054	0,023	0,067	0,068	0,049	0,012	0,094	0,098	0,077	0,021	0,020	0,021	0,018	0,006
	0,041	0,045	0,042	0,014	0,066	0,060	0,036	0,007	0,084	0,081	0,051	0,011	0,019	0,018	0,014	0,003

Note: Numerator - $\Delta_1 = f(300\text{ K})$, denominator - $\Delta_2 = f(2100\text{ K}) - f(900\text{ K})$.

Table 4 gives the calculated results for ²³⁹Pu mean-group cross-sections, and Table 5, the resonance self-shielding factor results as a function of temperature and dilution cross-section for the same nuclide. These calculations were made using the GRUKON program [9] which has a high

Table 4

Mean cross-sections for ^{239}Pu in the resolved resonance region, burns

Group No.	$E_n, \text{ eV}$	σ_t	σ_f	σ_c	σ_{ef}	Group No.	$E_n, \text{ eV}$	σ_t	σ_f	σ_c	σ_{ef}
16	215-465	41,9	13,1	13,3	15,5	22	2,15-4,65	24,4	11,5	4,8	8,1
17	100-215	52,5	19,6	17,5	15,4	23	1,00-2,15	35,5	23,4	3,6	8,6
18	46,5-100	115,6	57,0	40,4	18,2	24	0,465-1,00	149,6	99,5	40,3	9,8
19	21,5-46,5	69,0	22,8	34,4	11,8	25	0,215-0,465	2762,3	1699,0	1052,5	10,8
20	10,0-21,5	189,7	104,6	73,5	11,5	Ther-	0,0253	1019,6	744,0	269,1	6,5
21	4,65-10,0	68,6	33,8	27,0	7,8	mal					

level of accuracy thanks to the careful selection of the quadrature formulae for finite-difference integration. The following results were obtained. Group cross-sections on the whole agreed with the data given in Ref. [4], except for the data on $\langle\sigma_f\rangle$ and $\langle\sigma_c\rangle$ in groups 18 and 19. Note that the values obtained for $\langle\sigma_t\rangle$ were systematically higher those given in Ref. [4]. At the same time, the mean cross-sections obtained showed a high level of agreement with reliable primary experimental data on $\sigma_t(E)$ [10] and $\sigma_f(E)$ [11] used in the optimization procedure. The close agreement of the data obtained for $\langle\sigma_Y\rangle$ with the measurement results familiar from Ref. [12] should also be noted, though the latter were not taken into account in the evaluation process. Finally, the resonance self-shielding factors $f_t(\sigma_0)$ and $f_f(\sigma_0)$, at room temperature, proved to be very close to the values obtained by direct processing of the measurement results for the fission reaction transmission and self-indication functions [13]. At the same time, these results differ from those given in Ref. [4] in the same way as those for the unresolved resonance region (the evaluations obtained for $f_f(\sigma_0)$ and $f_c(\sigma_0)$ being systematically higher than the data in Ref. [4]).

When comparing the results obtained on temperature changes in the resonance self-shielding factors with those given in Ref. [4], differences analogous to those for the unresolved resonance region are evident. For the fission reaction, the calculated temperature increments for the intervals 900-300 K and 2100-900 K are systematically and significantly smaller than the

Table 5

Resonance self-shielding factors for ^{239}Pu , burns

Group No.	E_n, eV	T, K	$f_t(\delta_0)$					$f_f(\delta_0)$					$f_c(\delta_0)$					$f_{el}(\delta_0)$				
			0	10	10 ²	10 ³	10 ⁴	0	10	10 ²	10 ³	10 ⁴	0	10	10 ²	10 ³	10 ⁴	0	10	10 ²	10 ³	10 ⁴
16	215-465	300	0,486	0,522	0,669	0,902	0,987	0,570	0,623	0,788	0,951	0,994	0,351	0,412	0,640	0,911	0,989	0,810	0,827	0,888	0,970	0,996
		900	0,525	0,569	0,735	0,937	0,992	0,628	0,682	0,839	0,968	0,996	0,446	0,513	0,736	0,946	0,994	0,835	0,852	0,914	0,981	0,998
		2100	0,573	0,623	0,793	0,958	0,996	0,686	0,737	0,877	0,978	0,998	0,542	0,608	0,809	0,965	0,996	0,860	0,877	0,935	0,988	0,999
17	100-215	300	0,381	0,419	0,555	0,820	0,962	0,458	0,511	0,689	0,908	0,987	0,293	0,346	0,548	0,850	0,979	0,744	0,759	0,820	0,931	0,989
		900	0,399	0,443	0,604	0,866	0,980	0,493	0,551	0,737	0,934	0,992	0,350	0,411	0,629	0,897	0,987	0,758	0,776	0,844	0,950	0,993
		2100	0,426	0,476	0,656	0,901	0,984	0,539	0,599	0,783	0,932	0,994	0,415	0,481	0,698	0,928	0,991	0,775	0,795	0,868	0,964	0,996
18	46,5-100	300	0,213	0,241	0,365	0,654	0,927	0,328	0,375	0,552	0,824	0,970	0,199	0,230	0,369	0,701	0,946	0,579	0,597	0,666	0,831	0,968
		900	0,218	0,249	0,387	0,709	0,949	0,346	0,395	0,581	0,855	0,978	0,223	0,261	0,425	0,770	0,964	0,593	0,613	0,693	0,868	0,979
		2100	0,231	0,266	0,423	0,762	0,963	0,376	0,429	0,619	0,883	0,984	0,262	0,306	0,492	0,825	0,975	0,616	0,637	0,725	0,899	0,985
19	21,5-46,5	300	0,169	0,187	0,264	0,544	0,903	0,146	0,185	0,340	0,702	0,950	0,087	0,120	0,267	0,651	0,959	0,725	0,740	0,786	0,895	0,981
		900	0,170	0,190	0,280	0,612	0,931	0,155	0,198	0,376	0,755	0,963	0,098	0,138	0,313	0,722	0,958	0,728	0,745	0,800	0,918	0,987
		2100	0,173	0,196	0,307	0,683	0,951	0,169	0,220	0,425	0,806	0,973	0,115	0,164	0,372	0,785	0,970	0,734	0,753	0,817	0,937	0,991
20	10,0-21,5	300	0,096	0,114	0,202	0,507	0,888	0,147	0,186	0,346	0,690	0,943	0,105	0,136	0,278	0,643	0,934	0,803	0,806	0,831	0,912	0,983
		900	0,095	0,114	0,206	0,553	0,913	0,151	0,192	0,365	0,729	0,955	0,110	0,145	0,305	0,697	0,950	0,804	0,808	0,837	0,926	0,988
		2100	0,095	0,114	0,217	0,607	0,933	0,158	0,203	0,393	0,768	0,965	0,121	0,161	0,346	0,750	0,963	0,806	0,811	0,847	0,940	0,991
21	4,65-10,0	300	0,270	0,279	0,323	0,533	0,887	0,247	0,266	0,363	0,663	0,935	0,194	0,214	0,318	0,639	0,930	0,947	0,947	0,953	0,974	0,995
		900	0,270	0,279	0,325	0,567	0,909	0,249	0,269	0,377	0,701	0,949	0,197	0,218	0,333	0,679	0,945	0,947	0,948	0,954	0,977	0,996
		2100	0,271	0,279	0,330	0,611	0,928	0,254	0,276	0,399	0,743	0,960	0,201	0,225	0,356	0,725	0,957	0,947	0,948	0,955	0,980	0,997
22	2,15-4,65	300	0,987	0,991	0,998	1,00	1,00	0,985	0,990	0,997	1,00	1,00	1,00	1,00	1,00	1,00	1,00	0,999	0,999	1,00	1,00	1,00
		900	0,987	0,991	0,998	1,00	0,999	0,985	0,990	0,997	1,00	1,00	1,00	1,00	1,00	1,00	1,00	0,999	0,999	1,00	1,00	1,00
		2100	0,987	0,991	0,998	1,00	1,00	0,985	0,990	0,997	1,00	1,00	1,00	1,00	1,00	1,00	1,00	0,999	0,999	1,00	1,00	1,00
23	1,00-2,15	300	0,932	0,945	0,980	0,997	0,999	0,953	0,962	0,987	0,998	1,00	0,952	0,961	0,986	0,998	1,00	0,996	0,997	0,999	1,00	1,00
		900	0,931	0,945	0,980	0,997	0,999	0,953	0,962	0,987	0,998	1,00	0,952	0,961	0,986	0,998	1,00	0,996	0,997	0,999	1,00	1,00
		2100	0,931	0,944	0,980	0,997	0,999	0,952	0,962	0,987	0,998	1,00	0,952	0,961	0,986	0,998	1,00	0,996	0,997	0,999	1,00	1,00
24	0,465-1,00	300	0,556	0,575	0,684	0,905	0,988	0,720	0,736	0,820	0,953	0,994	0,611	0,633	0,748	0,933	0,992	0,966	0,968	0,979	0,995	0,999
		900	0,553	0,571	0,680	0,903	0,987	0,718	0,734	0,818	0,952	0,994	0,608	0,630	0,745	0,932	0,992	0,966	0,968	0,979	0,995	0,999
		2100	0,546	0,564	0,673	0,899	0,987	0,712	0,728	0,813	0,950	0,994	0,601	0,623	0,739	0,929	0,991	0,965	0,967	0,978	0,994	0,999
25	0,215-0,465	300	0,333	0,336	0,360	0,522	0,854	0,588	0,591	0,613	0,735	0,926	0,575	0,577	0,600	0,727	0,923	1,05	1,05	1,05	1,02	1,00
		900	0,342	0,345	0,369	0,534	0,863	0,601	0,603	0,625	0,747	0,931	0,588	0,591	0,613	0,738	0,928	1,05	1,05	1,05	1,03	1,00
		2100	0,361	0,364	0,390	0,559	0,878	0,626	0,628	0,650	0,767	0,939	0,614	0,617	0,639	0,760	0,937	1,06	1,06	1,05	1,03	1,01

values given in Ref. [4]. For the capture reaction, analogous differences may be observed in energy groups 18 and 21; in the remaining groups the difference is not so great. This shows that calculating the Doppler effect for ^{239}Pu on the basis of the data given in Ref. [4] leads to significant overestimation of that effect.

These results demonstrate the potential of the new programs developed by the Power Physics Institute for analysing neutron data and preparing group constants using evaluated resonance parameters within a multilevel formalism. These programs are of practical importance, particularly for the self-consistent calculation of group constants for fissile nuclei (in an arbitrary group representation) in the resolved and the unresolved resonance regions. The group constant evaluations obtained fill a gap in the data given in Ref. [4] for ^{233}U , and for ^{235}U and ^{239}Pu they show how data must be adjusted, particularly data on resonance self-shielding factors and their temperature dependence.

REFERENCES

- [1] VAN'KOV, A.A., TOSHKOV, S.A., UKRAINTSEV, V.F., et al., Method for analysing transmission functions and neutron cross-sections in the unresolved resonance region for heavy nuclides, Preprint OIYaI [Joint Nuclear Research Institute] No. 3-84-848, Dubna (1984) [in Russian].
- [2] KOLESOV, V.V., LUK'YANOV, A.A., Neutron absorption cross-section for ^{239}Pu in the resolved resonance region, At. Ehnerg. 58 3 (1985) 197-198 [in Russian].
- [3] KOLESOV, V.V., LUK'YANOV' A.A., Multilevel analysis parameters for ^{239}Pu cross-sections in the resonance region, Preprint FEhI-1404 [Power Physics Institute], Obninsk (1983) [in Russian].
- [4] ABAGYAN, L.P., BAZAZYANTS' N.O., NIKOLAEV, M.N., TSIBULYA, A.N., Group Constants for Reactor and Protection Calculations, Ehnergoizdat, Moscow (1981) [in Russian].
- [5] KIKUCHI, Y., Evaluation of neutron nuclear data for ^{233}U in thermal and resonance region: Rep. JAERI-9318 (1981).
- [6] BHAT, M.R., Evaluation of ^{235}U neutron cross-section data for ENDF/B-V: Rep. BNL-NCS-51184, Brookhaven (1980).

- [7] VAN'KOV, A.A., GOSTEVA, L.S., UKRAINTSEV, V.F., et al., Measurement of transmission functions and evaluation of mean resonance parameters and group constants for ^{235}U in the unresolved resonance region, Vopr. At. Nauki i Tekhniki, Ser. Yad. Konstanty 1 (1985) 35-41 [in Russian].
- [8] VAN'KOV, A.A., TOSHKOV, S.A., UKRAINTSEV, V.F., et al., Group cross-sections and resonance self-shielding factors for ^{239}Pu in the unresolved resonance region, *ibid.* 4(53) (1983) 18-25 [in Russian].
- [9] SINITSA, V.V., The GRUKON package, Preprint FEhI-1188, Obninsk (1981) [in Russian].
- [10] DERRIEN, H., BLONS, J., EGERMANN, C., et al., Sections efficaces totales et de fission du ^{239}Pu - etude statistique des parameters de resonances - In: Nucl. Data for reactors, Proc. of IAEA conf. (Paris, 1966) Vol. 11, IAEA, Vienna (1967) 195.
- [11] BLONS, J., High resolution measurements of neutron-induced fission cross-sections for ^{233}U , ^{235}U , ^{239}Pu and ^{241}Pu below 30 keV, Nucl. Sci. and Eng. Vol. 51, 2 (1973) 130.
- [12] GWIN, R., INGLE, E.G., WEAVER, H., Measurements of the neutron capture and fission cross-section of ^{239}Pu and ^{235}U , 0.02 eV to 200 keV, the neutron capture cross-sections to ^{197}Au , 10 to 50 keV and neutron fission cross-section of ^{235}U , 5 to 200 keV, *ibid.* Vol. 59, 2 (1976) 79.
- [13] BAKALOV, T., VAN'KOV, A.A., GRIGOREV, Yu.V., et al., Transmission and self-indication measurement for ^{235}U and ^{239}Pu in the 2 eV-20 keV neutron energy region, Preprint OIYaI RZ-12796, Dubna (1979) [in Russian].